1993

Reactive ion etching of Si/SiO2 by CHF3/CH4/O2 gas mixture

Usha Raghuram
San Jose State University

Order Number 1353052

Reactive ion etching of Si/SiO_2 by $CHF_3/CH_4/O_2$ gas mixture

Raghuram, Usha, M.S.

San Jose State University, 1993

U·M·I
300 N. Zeeb Rd.
Ann Arbor, MI 48106

REACTIVE ION ETCHING OF Si/SiO_2 BY $CHF_3/CH_4/O_2$ GAS MIXTURE

A Thesis Presented to

The Faculty of the Department of Materials Engineering

San Jose State University

In Partial Fulfillment of

the Requirements for the Degree

Master of Science

by

USHA RAGHURAM

May 1993

APPROVED FOR THE DEPARTMENT OF MATERIALS ENGINEERING

P S Gwozdz 2/19/93

Dr. Peter Gwozdz, Thesis Advisor
Center for Electronic Materials

2-18-93

Dr. K. Sree Harsha, Reading Committee Chairman
Department of Materials Engineering

Melanie McNeil 2-18-93

Dr. Malanie McNeil, Reading Committee Member
Department of Chemical Engineering

2/18/93

Dr. Karen Singmaster, Reading Committee Member
Department of Chemistry

APPROVED FOR THE UNIVERSITY

M. Jon Lewandowski

ABSTRACT

REACTIVE ION ETCHING OF Si/SiO_2 BY $CHF_3/CH_4/O_2$ GAS MIXTURE

by Usha Raghuram

The reactive ion etching of silicon and silicon dioxide by the gas mixture $CHF_3/CH_4/O_2$ was studied using an AME-8110 RIE etcher. Five process variables were varied: bias, pressure, and flow rates of CHF_3, CH_4, and O_2. The etch rates of SiO_2 and Si were measured. The selectivity of oxide etching relative to silicon was analyzed. It was found that the addition of methane increased the selectivity. The maximum selectivity obtained was 24. The influence of the variables was obtained by a second order regression analysis of the data. The observed effects are consistent with the analysis based on published reports.

ACKNOWLEDGEMENTS

I would like to thank Professor Peter Gwozdz for his valuable guidance at all stages of this work. He was a constant source of support and encouragement. The suggestions of Professors K. Sree Harsha, Melanie McNeil, and Karen Singmaster, starting from the thesis proposal stage, were very helpful. My thanks are also due to Mr. John Strazynski for his assistance in the lab work.

None of this would have been possible but for the support of my husband, parents-in-law, and son in the home front.

TABLE OF CONTENTS

1. INTRODUCTION 1

2. PLASMA ETCHING - AN OVERVIEW 4
2.1. Plasma Production and Reactor Design 4
2.2. Plasma Reactions and Variables that Influence Etching 6
2.3. DC Bias/ RF Power Control 10
2.4. Evaluation of Plasma Processes 12

3. ETCHING BY FLUOROCARBONS - A REVIEW 15
3.1. Etching by CF_4 Plasma - Effect of Oxygen Addition 15
3.2. Effect of Hydrogen Addition to CF_4 Plasma . 16
3.3. Fluorocarbons with varying Carbon/Fluorine Ratios 19
3.4. Etching by CHF_3 20
3.5. Effect of CHF_3 and CH_4 Addition to CF_4 . . . 21
3.6. Effect of CH_4 Addition to CHF_3 and CF_4 . . . 21
3.7. CO_2 Addition to CHF_3 22
3.8. Mechanism of Etching by Fluorocarbon Plasmas 23
3.9. Effect of Process Variables 25
3.9.1. Effect of DC Bias 25
3.9.2. Effect of Pressure 26
3.9.3. Effect of CHF_3 and CH_4 27
3.9.4. Effect of Oxygen 27
3.10. Justification for the Current Work 27

4. EXPERIMENTAL PROCEDURE 29
4.1. Wafer Preparation 29
4.1.1. Thermal Oxidation of Si Wafers . . . 29
4.1.2. Photolithographic Processing 29
4.1.3. Oxide Etch and Resist Stripping . . . 30
4.2. Plasma Etching 31
4.3. Measurement of Oxide Etch Rate 34
4.4. Measurement of Silicon Etch Rate 34
4.5. Variable Ranges 35
4.6. Regression Analysis 37
4.7. Change in Power Requirements 38

5. RESULTS 39
5.1. Second Order Analysis in the Narrow Range . 39
5.2. Second Order Analysis in the Expanded Surface 41
5.3. Summary 42

6. DISCUSSION 44
6.1. Selectivity 44
6.2. SiO_2 and Si etch Rates 49
6.3. Influence of Variables 55
6.4. Reliability of the Observed Trends 60
6.5. Summary 62

CONCLUSIONS 63

REFERENCES 64

APPENDIX 1 67

APPENDIX 2 69

APPENDIX 3 88

APPENDIX 4 89

LIST OF TABLES

1. Effect of C/F Ratio on SiO_2/Si Selectivity 21
2. Variables and their Initial Ranges 36
3. Narrow Variable Ranges 36
4. Expanded Reaction Surface 37
5. Etch Rates and Selectivities for the Second Order Fit in the Narrow Range 40
6. Second Order Regression Analysis in the Narrow Range 41
7. Second Order Regression Fit of Expanded Reaction Surface 41
8. Additional Data in the Expanded Surface used in Second Order Fit 42
9. Effect of Methane Addition 46
10. Influence of Variables 55
11. F-Ratios of the Regression Analysis of The Etch Rates and Selectivity 62

LIST OF FIGURES

1. Plasma Production by a DC Discharge 5
2. RF Plasma Discharge 6
3. Electrode Arrangement in Direct, Capacitive, and Inductive Coupling Modes 7
4. Layout and Section View of NMOS Inverter 8
5. [F·] vs [O_2] 17
6. Si Etch Rate vs. [F·] 18
7. SiO_2 Etch Rate vs. [F·] 18
8. Etch Rate vs. %H_2 19
9. Etch Rate vs. %O_2 22
10. Etch Rate vs. %CHF_3 22
11. Etch Rate vs. % CH_4 in CF_4 23
12. Effect of Methane Addition to CHF_3 23
13. Pattern of Oxide over Silicon 30
14. Schematic Diagram of an AME-8110 RIE System . . . 33
15. Effect of Negative Bias, X1, on Selectivity . . . 46
16. Effect of Pressure, X2, on Selectivity 47
17. Effect of CHF_3 Flow Rate, X3, on Selectivity . . . 47
18. Effect of CH_4 Flow Rate, X4, on Selectivity . . . 48
19. Effect of O_2 Flow Rate, X5, on Selectivity 48
20. Effect of Negative Bias, X1, on the Oxide Etch Rate 50
21. Effect of Pressure, X2, on the Oxide Etch Rate . . 50
22. Effect of CHF_3 Flow, X3, on the Oxide Etch Rate . 51
23. Effect of CH_4 Flow, X4 (sccm), on the Oxide Etch Rate 51
24. Effect of O_2 Flow, X5 (sccm), on the Oxide Etch Rate 52
25. Effect of Negative Bias, X1, on the Si Etch Rate . 52
26. Effect of Pressure, X2, on the Si Etch Rate . . . 53
27. Effect of CHF_3 Flow, X3, on the Si Etch Rate . . . 53
28. Effect of CH_4 Flow, X4 (sccm), on the Si Etch Rate 54
29. Effect of O_2 Flow, X5 (sccm), on the Si Etch Rate 54

1. INTRODUCTION

Integrated circuit (IC) chips with a million components are commonplace in current technology. Very large scale integration (VLSI) in the chips is achieved by the miniaturization of the devices to submicron dimensions. Many IC fabrication processes involve the sequential formation of patterned layers of materials on the wafer surface. IC chips with submicron features require anisotropic pattern transfer. Conventional wet etching is isotropic, i.e., the pattern etched is wider than the original hole. Anisotropy can be obtained by dry etching when the wafers are exposed to the electric field as in the case of reactive ion etching (RIE). RIE and other plasma etching processes are discussed in detail in many books[1,2] and review articles[3,4]. Chapter 2 provides a short review of plasma etching and can be skipped by an individual who is familiar with the subject.

Contact holes to silicon and via holes between various levels of interconnect in multilevel metallizations are made by the anisotropic etching of silicon dioxide, SiO_2. Hard baked photoresists are used to create the patterns. The vast majority of dry etching processes for silicon dioxide are based on fluorocarbon (Freon) discharges. Selectivity to silicon is another crucial factor in the processing of

silicon dioxide. Plasma etching of silicon and silicon dioxide by Freons is well documented[5,6]. Fluorine atoms are responsible for the etching of silicon. The etch rates are lower by 1-2 orders of magnitude for atomic fluorine etching of silicon dioxide. In fluorine deficient plasmas, HF and polymer film formation retard silicon etch rates. Oxide etch rates can be enhanced by ion bombardment. Chapter 3 provides a summary of silicon and its oxide etching in fluorocarbon plasmas.

Practical processes in use nowadays use Freon-23 (trifluoromethane), almost exclusively, in combination with additives such as Ar or He for the selective patterning of silicon dioxide. The effect of addition of methane (CH_4) to trifluoromethane (CHF_3) on the etch rates and selectivity for oxide etching relative to silicon in the reactive ion etching of silicon and silicon dioxide was examined in this study. From a review of relevant literature, presented in Chapter 3, it was postulated* that CHF_3/CH_4 plasma would lead to lower etch rates for silicon and higher selectivity for silicon dioxide etching. Oxygen was found to be

*The authors were unaware of the work of Norstrom et al.[17] when the effect of addition of CH_4 to CHF_3 was hypothesized. The results obtained in this study are consistent with the observations of Norstrom et al.

necessary to prevent polymerization on the wafer surface and on the walls of the reaction chamber.

Chapter 4 describes the experimental procedures for wafer preparation, RIE etching, and etch rates and selectivity measurements. It was proposed to use the response surface methodology, RSM, in the design of experiments. As can be seen from the literature, maximum in selectivity occurs near the polymer point. Hence, data could not be collected under some conditions close to the polymer point. So, conventional experimental designs for the RSM approach could not be used close to the maximum in selectivity. The experimental design is discussed in Chapter 5. The variables were bias, pressure, and flow rates of trifluoromethane, oxygen, and methane.

The results and discussions are presented in Chapters 6 and 7 respectively. The initial hypothesis which led to this project--methane addition decreases silicon etch rates and increases SiO_2/Si etching selectivity--was confirmed.

2. PLASMA ETCHING - AN OVERVIEW

Plasma etching is a very commonly used technique in the production of IC chips and multichip modules. With increasing circuit density and narrower line width requirements, anisotropic etching became necessary to pattern features smaller than 2-3 microns. Plasma etching offered not only anisotropic etching but also replaced corrosive liquids by safe nontoxic gases such as O_2 and CF_4 and made the processes simple and suitable for automation.

2.1. Plasma Production and Reactor Design

A plasma is a neutral collection of electrons, positive and negative ions, neutral species such as free radicals, excited molecules and molecular fragments. In plasma etching applications, plasmas are produced in the reaction chamber by an electric field that induces the ionization of the gas at pressures less than 1 Torr[1].

Plasmas can be generated by either a DC or an AC voltage or by a DC bias in conjunction with a high-frequency discharge[1]. Figure 1 illustrates the generation of a plasma by a DC glow discharge. A schematic representation of an RF plasma discharge where the power is supplied to the RF cathode through a matching network is given in Figure 2.

Figure 2b shows the average DC negative potential of the two electrodes and the plasma. The negative potential of the cathode relative to the anode is a consequence of the smaller cathode area. If the two electrodes were equal in area, then both the electrodes will be at the same potential due to symmetry[1].

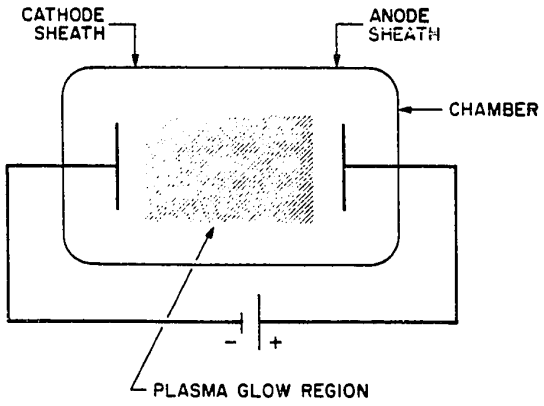

Figure 1. Plasma Production by a DC Discharge

Etchers can be operated on three different modes, namely, direct, capacitive and inductive coupling modes. In the direct coupling mode, there is a free exchange of charge between the plasma and the conducting layer. In the capacitive coupling mode, a dielectric separates the two. In the inductive coupling, a changing magnetic field induces an alternating voltage that sustains the discharge. Figure 3 shows the electrode arrangements in the three modes[5].

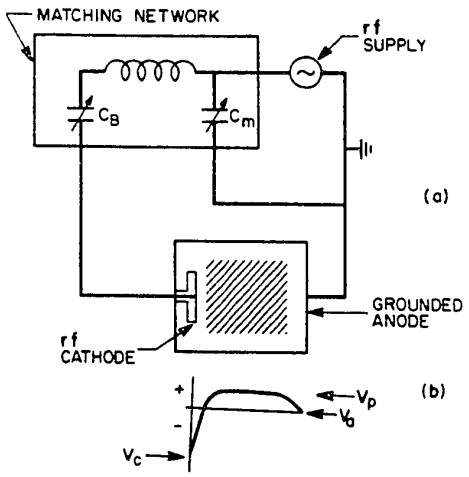

Figure 2. RF Plasma Discharge

Depending on the pressure of the gas in the reaction chamber, the frequency of the RF discharge, the applied power, and the bias of the wafers, plasmas can be utilized in a variety of capacities[2]. For example, in reactive ion etchers(RIE) and planar plasma etchers(PPE), the electrode is capacitively coupled to a RF generator and will have a negative potential with respect to the plasma. In the RIE mode, the wafers are loaded on to the cathode; in the PPE mode, the wafers are on the grounded electrode. An illustrative diagram and a brief description of an AME-8110 RIE etcher is given in Section 4.2.

2.2. Plasma Reactions and Variables that Influence Etching

Due to the presence of various layers such as Si, SiO_2, Si_3N_4, metallization materials, the patterning of an IC

device is complicated and require fine lines (1-2 μm) as seen from the example in Figure 4. In addition, in reactive ion etchers, the cations in the plasma are accelerated by the potential before striking the cathode on which the wafers are loaded. These energetic ion bombardments cause further reactions in the substrate, and are helpful especially in the etching of SiO_2.

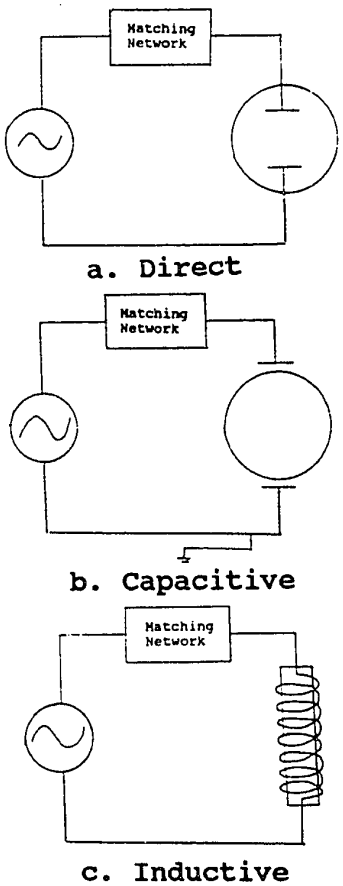

Figure 3. Electrode Arrangement in Direct, Capacitive, and Inductive Coupling Modes

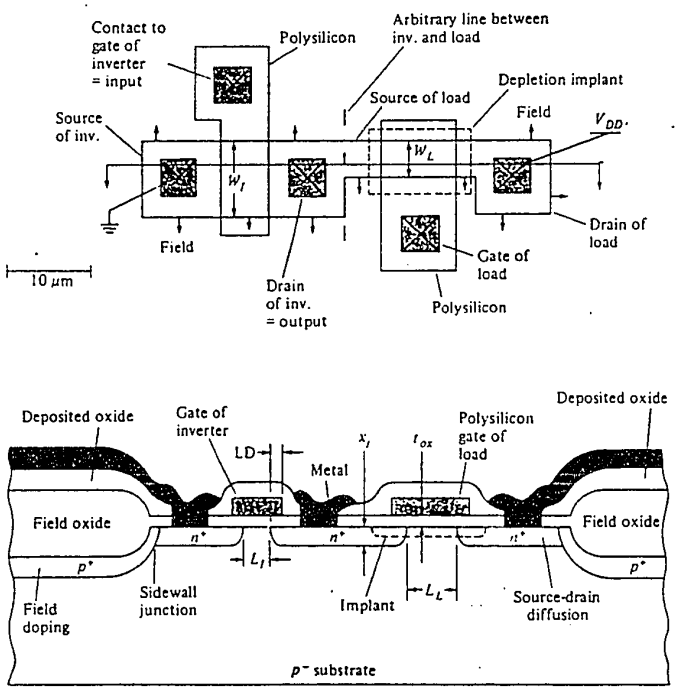

Figure 4. Layout and Section View of NMOS Inverter

In order to use plasma etching processes effectively in the fabrication of IC devices, the process requirements are quite stringent. Some of the etching characteristics that play a crucial role in the choice of a process are:

i) Etch Rate: The etchant must be able to etch the layer of interest at rates high enough (about few hundred A/min) to make the process economically viable.

ii) Selectivity: Selectivity defines relative material etching rates in a plasma. The etch rates of layers other than the one of interest should be zero or very small. In other words, the etchant and the reaction

conditions should be chosen in such a way that the layer of interest is etched selectively with minimum disruption to other layers.

iii) Uniformity: The etch rate should be uniform across the wafer and from wafer to wafer.

iv) Anisotropy: Anisotropy is the ratio of the difference between the vertical and the horizontal etch rates to the vertical etch rate. Although, in many processes an anisotropy of 1 is required, there are some processes which require an intermediate anisotropy, i.e., between 0-1.

v) Resolution and Taper Angle: Anisotropy is responsible for dimension control since it exerts influence over factors such as resolution, and taper angle. Resolution is the factor that controls how narrow a line can be. Taper angle is a measure of the slope of the edges or the edge profile.

Fluorinated and chlorinated hydrocarbons and compounds of boron, nitrogen, and sulfur are some of the etchants used for the reactive ion etching of the substrate layers such as Si, polysilicon, SiO_2, Si_3N_4, refractory gate metals, their silicides, and photoresist[1]. Simple gases such as F_2 and Cl_2 etch silicon but not silicon dioxide. Selective etching of silicon dioxide is required in some fabrication processes

and is generally achieved by the use of fluorinated compounds. Oxide etch rates are increased by energetic ion bombardment.

Variations in the etchants and additive gases have influence over the etching characteristics such as the etch rate, selectivity, resolution, uniformity, and anisotropy[1]. For example, by adding up to 15% of O_2 to CF_4 Si/SiO_2 selectivity can be increased since 5-6 fold increase is induced in the Si etch rate while the SiO_2 etch rate is increased only slightly[2].

Anisotropy exerts influence over pattern transfer by controlling the undercut and edge profile. Good anisotropy can be obtained by ion assistance and by sidewall mechanism[1]. In ion assisted etching, since the direction of acceleration of the ions across the sheath potential is perpendicular to the electrode surface, the ions strike the wafers at 90° and lead to preferential etching. Build up of polymer film along the sides protect those sides from being etched and this process is called the sidewall mechanism.

2.3. DC Bias/ RF Power Control

It was seen in the previous section that ion bombardment is responsible for the selective etching of silicon dioxide.

The important process parameters that control ion energies are RF power and DC bias. An increase in RF power at constant pressure increases the ion energies by increasing the potential across the ion sheath. The RF power determines the degree of ionization. However, the number of ions striking the wafer is not only controlled by power but also by the reactor design. For this reason, processes conducted in different instruments can not be compared. Many reports use power density as a process parameter[5]. On the other hand, DC bias, being a direct measure of the ion energies, is a better variable to control and compare processes[6]. Moreover, it has been shown that in commercial etching equipment there can be high power losses which render the comparison of power dissipation in the plasma difficult[7].

It was observed in our laboratories and by the Applied Materials Engineers that power requirements to maintain a constant bias under identical process conditions varies for the same equipment on a day to day basis. It was noted that these variations in power did not affect the etch rates[8]. For these reasons, DC bias was chosen as a variable in our study instead of power. However, in the present study, though the same Applied Materials etcher was used, changes in power requirements did lead to changes in etch rates.

2.4. Evaluation of Plasma Processes

To control the etching process it is important to understand the reaction mechanism. The relative volatilities and vapor pressures of various etch products influence the concentrations of the species at the reaction site, and hence affect the kinetics. The relative bond strengths of silicon-silicon, silicon-oxygen, silicon-halogen, metal-metal, and metal-silicon bonds are the thermodynamic parameters that control the dynamics of etching of various substrates constituting the IC device[3]. For example, Si-O bonds are stronger than Si-Si bonds. The bond energy of a Si-O bond is 185 kcal/mole while that of a Si-Si bond is only 42 kcal/mole. Due to the high bond energy of the Si-O bond SiO_2 is chemically very inert and it is very difficult to selectively etch SiO_2. In plasma etching processes, SiO_2 is etched by the fluorocarbon plasmas in the RIE mode wherein ion assistance is provided for etching. Since F atoms, the etching species for silicon, are also present in fluorocarbon plasmas, Si etch rates should be suppressed in order to obtain selectivity in SiO_2 etching. In situ formation of a hydrocarbon film on the substrate and hydrogen fluoride (HF) in the fluorocarbon plasmas retard silicon etching. Hence, an understanding of the reaction mechanism is helpful in interpreting the relative etch rates and selectivities, and is crucial in process control.

To selectively etch a single layer or multiple layers of thin films over underlying layers of etchable substrates, the ability to detect the end point is essential. Some of the methods used are mass spectrometry, optical emission and reflection methods, and Langmuir probe[1]. In mass spectrometry, choosing the ion to be monitored is important for proper end-point detection. This is due to the fact that the molecules that enter the mass spectrometer are not only ionized but also fragmented. More than one compound may produce the same ion. Hence, the ion chosen should be characteristic of the molecule of interest and should not be formed from any other species present in the effluent mixture of the plasma process.

Plasma etching can be effectively utilized in obtaining fine-line patterns required in VLSI fabrication. However, due to the complexity of device structures, processing also becomes more complex and requires careful monitoring. Factors such as mechanism of etching, end-point detection, advantages and trade offs should be well understood for evaluating a process. Hence, a good process design would require a thorough understanding of the processes involved and judicious manipulation of the process variables and reactor design. A detailed study of the relevant reports available would be beneficial for establishing a good

process design. In the next chapter the mechanism of plasma etching by fluorocarbons is reviewed in order to evaluate the influence of the addition of methane on the etching behavior of trifluoromethane.

3. ETCHING BY FLUOROCARBONS - A REVIEW

Fluorinated and chlorinated hydrocarbons, and compounds of boron, nitrogen, and sulfur are some of the etchants used for reactive ion etching of Si, SiO_2, Si_3N_4, gate material such as refractory metals and their silicides, photoresist and other layers constituting the IC device.[1] Fluorocarbon discharges are used in the majority of oxide etching processes[6]. In our study, RIE etching of SiO_2 and Si was examined using the gas mixture $CHF_3/CH_4/O_2$. From the review presented in this chapter, the mechanism of etching by this gas mixture can be understood.

3.1. Etching by CF_4 Plasma - Effect of Oxygen Addition

Plasma etching of Si layers is most commonly done using CF_4/O_2 mixture in semiconductor fabrications. For device fabrication the silicon to be etched can be that of a wafer (single crystal) or a layer of polysilicon used for MOS gate arrays. The etching normally requires selectivity to favor a fast etch rate for Si with minimum loss of the SiO_2 substrate[2]. Si is etched selectively over SiO_2 by CF_4 plasma when small amounts of oxygen are added to the feed gas[9]. The main reactions controlling the etching of silicon by CF_4 are:

$$e + CF_4 \longrightarrow CF_3^+ + F\cdot + 2e$$

$$e + CF_4 \longrightarrow CF_3^{\cdot} + F^{\cdot} + e$$

$$Si + 4F^{\cdot} \longrightarrow SiF_4$$

$[F^{\cdot}]$ determines the rate and hence, the equilibrium constant was approximated[10] by $K = [F^{\cdot}] \times [CF_3] / [CF_4]$.

Mogab et al.[9] characterized the plasma reactions in CF_4-O_2 by means of emission spectroscopy, mass spectrometry, infrared spectroscopy, and etch rate measurements. They observed that the fluorine atom concentration in the plasma reached a maximum at an oxygen content of 23.6% as noted in Figure 5. They attributed this to two sets of opposing reactions, both sets occurring homogeneously and heterogeneously: One was the reduction in reactivity of $F^{\cdot}$ due to competing oxygen while the other was the reaction of oxygen with fluorinated species liberating $F^{\cdot}$. Figures 6 and 7 represent the effect of $[F^{\cdot}]$ on the etch rates of Si and SiO_2. The etch rate of Si did not increase monotonically with $[F^{\cdot}]$ due to competition by oxygen. SiO_2 etch rates were low and showed approximately linear dependence on $[F^{\cdot}]$.

3.2. Effect of Hydrogen Addition to CF_4 Plasma

Fluorine atoms are responsible for the etching of Si. CF_3 radicals and ions are adsorbed on the Si surface and form a thin polymer film. This film retards the etching of Si.

Added oxygen removes this film and increases Si etch rate. Addition of hydrogen to CF_4 plasma reduces Si etch rate by HF formation[11]. However, SiO_2 etching continued even in a fluorine deficient discharge because of the presence of radicals such as CF_3. Hence, the addition of hydrogen to CF_4 leads to an increase in selectivity of SiO_2 with respect to Si, as shown in Figure 8. Maximum selectivity of 30 was observed at 40% of H_2 in CF_4. Beyond 40% H_2, polymerization took place on the cathode surface. In SiO_2, the polymer film was removed by the following reaction:

$$SiO_2 + CF_3 \text{ ------> } SiF_4 + CO + CO_2 + COF_2$$

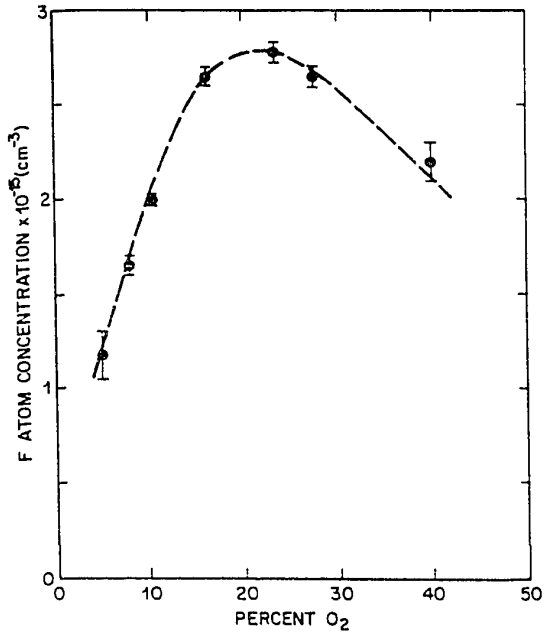

Fig 5. [F·] vs [O_2]

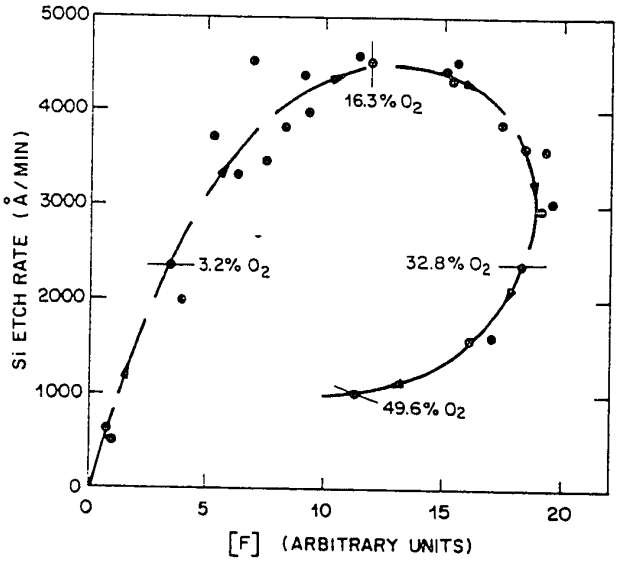

Fig 6. Si Etch Rate vs. [F·]

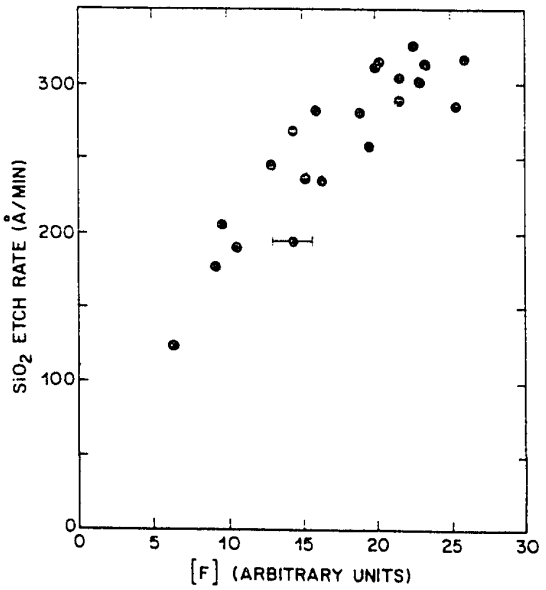

Fig. 7. SiO_2 Etch Rate vs. [F·]

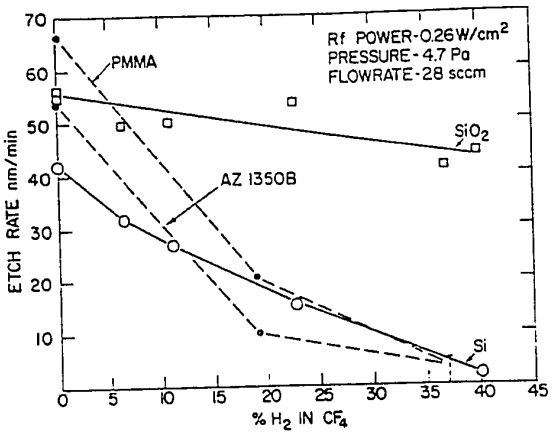

Fig. 8. Etch Rate vs. $\%H_2$

The difference in the rates of SiO_2 etching by CF_4 obtained by Mogab and Ephrath, namely, 100 and 500 Å/min respectively, is due to the different modes of etching. The work of Mogab et al.[9] was in the plasma etching mode; however, Ephrath's work[11] was with a reactive ion etcher. In the latter mode SiO_2 etching was assisted by ion bombardment which enhanced the etch rate.

3.3. Fluorocarbons with varying Carbon/Fluorine Ratios

Heinecke[12] was able to increase the selectivity of SiO_2 by changing the C/F ratio of the etchants as shown in Table 1. However, in the reactive ion beam etching (RIBE) mode the C/F ratio did not have comparable influence on selectivity[13]. Reactive ion beam etching, RIBE, differs from ion milling in that the impinging ion beam consists of

chemically reactive ions which upon striking the surface remove material by a combination of ion bombardment and chemical reaction.

In CHF_3, HF formation is another factor that increases the SiO_2 selectivity. In the RIBE mode, dramatic increase in SiO_2 etch rates were observed with increase in ion energy[13]. This supports the assistance by energetic ion bombardment in SiO_2 etching. Increase in Si etch rates were attributed to the removal of polymer films by ion bombardment at higher current densities. Due to ion assistance in etching, good anisotropy was obtained.

3.4. Etching by CHF_3

Light and See[14] correlated the etch rates and selectivities in SiO_2/Si removal by CHF_3 to the ratio of pressure to flow rate ratio(P/F). For reactive species, P/F ratio is proportional to the residence time of the species. Increase in P/F ratio led to increase in the Si etch rate. Maximum selectivities of 10-20 for SiO_2 were observed when P/F was less than 2. The process yielded good anisotropic etching. Formation of HF and ion assistance were the causes for the observed etch rate and selectivity. In CHF_3 etching, addition of oxygen was reported to reduce the selectivity of SiO_2 to Si while increasing the uniformity[15].

Table 1. Effect of C/F Ratio on SiO_2/Si Selectivity

Etchant	C/F Ratio	SiO_2/Si Selectivity	
		Plasma Etch[12]	RIBE[13],*
CF_4	1/4	1	6
C_2F_6	1/3	3	7.5
C_3F_8	1/2.7	5	7.5
CHF_3	1/2	10	-

*Etch rates at 750eV taken from the plots of ion energy versus etch rates for various etchants were used to compute the selectivity.

3.5. Effect of CHF_3 and CH_4 Addition to CF_4

The addition of CHF_3 or CH_4 to CF_4 yielded good selectivity in SiO_2 etching compared to NbN as shown in Figures 9-11[16]. The formation of HF led to a decrease in NbN etch rate. Since the process involved RIE, ion bombardment caused SiO_2 etching. The edge profiles obtained in CF_4/O_2 etching was poor and undercut in comparison with other mixtures.

3.6. Effect of CH_4 Addition to CHF_3 and CF_4

Polymer formation is used to increase the selectivity in the RIE etching of SiO_2 relative to Si by the addition of CH_4 to CHF_3[17]. Methane was shown to retard the etch rates of SiO_2, Si, and Si_3N_4. Figure 12 represents the dependence of the etch rates on the amount of CH_4 in CHF_3. A selectivity of 15 was obtained by using 2% CH_4 in CHF_3. Resist erosion was also found to be minimized by the addition of CH_4 to CHF_3.

It was suggested that infinite degree of selectivity in SiO_2 etching could be achieved by admixing minor amounts of CH_4 to CHF_3. The importance of carbon deposition and oxygen release from SiO_2 was demonstrated by using various cathode materials and by sputter etching in an argon atmosphere.

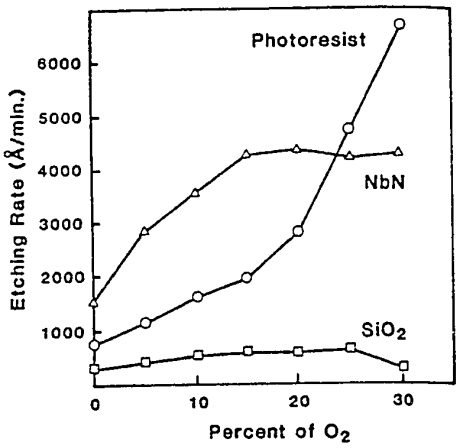

Fig. 9. Etch Rate vs. $\%O_2$

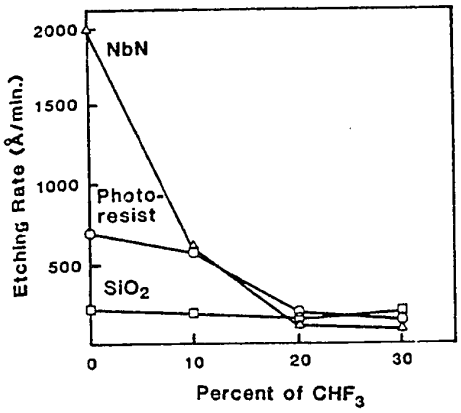

Fig. 10. Etch Rate vs. $\%CHF_3$

3.7. CO_2 Addition to CHF_3

A selectivity of over 25 was obtained for SiO_2 with respect to polysilicon by adding up to 3% CO_2 to CHF_3 in the RIE etching[18,19]. However, selectivity in the etching of SiO_2 relative to the photoresist was decreased in this mixture. The oxide etch rates as well as uniformity in etching decreased with increases in pressure and flow rates of CHF_3 and was attributed to increased polymerization[19]. CO_2 was found to be less effective in reducing the polymer formation

in relation to O_2[20]. However, CO_2 addition decreases the selectivity of oxide etch with respect to silicon and resist etches to a much lesser extent in comparison with O_2.

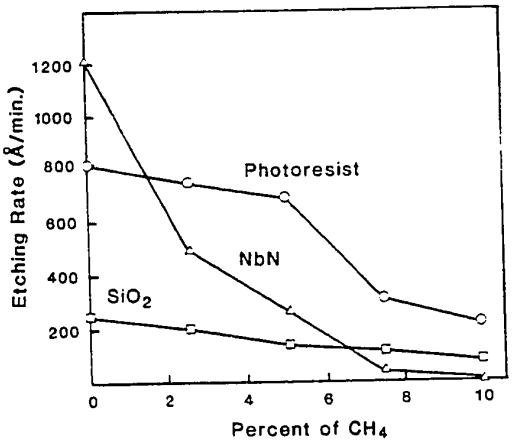

Fig. 11. Etch Rate vs. % CH_4 in CF_4

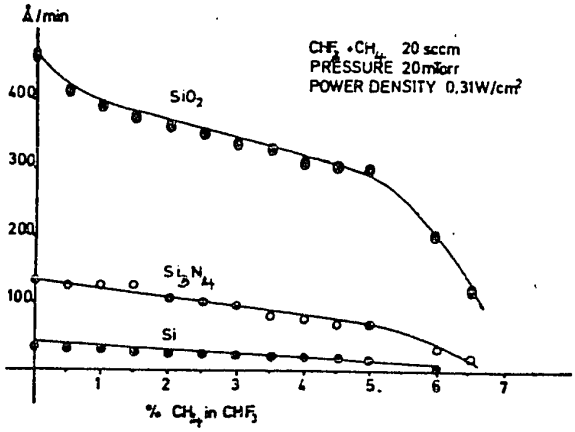

Figure 12. Effect of Methane Addition to CHF_3

3.8. Mechanism of Etching by Fluorocarbon Plasmas

The etching species for Si and SiO_2 in fluorocarbon plasmas is the fluorine atom produced by the dissociation of the

fluorocarbon[21]. The etch rates for SiO_2 etching by fluorine radicals are about 1-2 orders of magnitude lower than Si. Ion assistance is the major factor that increases the etch rate of SiO_2. Selectivity in the etching of SiO_2 can be increased by a decrease in fluorine atom concentration and an increase in polymerization.

Formation of HF reduces the fluorine atom concentration in the plasma[22]. HF does not react with Si. However, it reacts with SiO_2 and produces SiF_4 and H_2O according to the following reaction.

$$SiO_2 + 4HF \longrightarrow SiF_4 + H_2O$$

HF formation can be enhanced by the addition of gases such as H_2[11], CH_4[17], and C_2H_2[23].

Fluorine deficiency can also be caused by a decrease in fluorine to carbon ratio. Gases such as C_2F_6, C_3F_8 have lower F/C ratio relative to CF_4 and etching by these gases lead to higher selectivity in oxide etching[12,13]. Unsaturated fluorocarbon radicals and oligomers derived from them are the precursors to the inhibitor sidewall film that promote anisotropic etching. Unsaturated fluorocarbon polymers also consume the fluorine radicals for saturation. Difluorocarbene radicals formed from the fluorocarbon feed gas are the precursors for polymer films[24,25]. The main

reaction occurring in the CHF_3 plasma is[26]:

$$CHF_3 + e \longrightarrow CF_2 + HF$$

In plasmas with high C/F ratios, the concentrations of CF_2 and CF radicals are higher and hence, are the probable etchant species. When adsorbed on the oxide surface, these radicals can form a carbon containing film that persist during etching. SiO_2 acts as an oxygen supplier to burn off these polymer films in the presence of ion bombardment[17,27]. Since there is no mechanism by which the polymer film can be removed from the Si surface, the build up of polymer on the silicon surface is greater and this leads to the decreased Si etch rates and increased SiO_2 selectivity.

3.9. Effect of Process Variables

Process variables affect the etching characteristics either by changing the concentrations of reactive species, or by influencing the polymer deposition or by varying the ion energies. Trends noted in this section were also observed in our studies.

3.9.1. Effect of DC Bias:

Increase in bias leads to an increase in oxide etch rates as well as silicon etch rates. In a CHF_3/O_2 plasma, at low oxygen contents, the fluorine atom concentration is low.

Under these conditions, the oxide etching is either direct reactive ion etching, that is, ions themselves are the etching species[28], or ion assisted etching by fluorocarbon radicals[27]. Increase in bias would lead to increased ion energies and thereby increase the oxide etch rate. The deposited carbonaceous film on the silicon surface would also erode due to ion bombardment and hence, silicon etch rates would also increase with bias.

3.9.2. Effect of Pressure:

Degree of ionization in plasmas is generally independent of the operating pressure. However, increase in pressure leads to an increase in quenching rate of the radicals which is a consequence of the decrease in the mean free path of the species. Hence, the concentration of neutral species such as $F^{\cdot}$ decreases while that of the unsaturates increases[5]. Due to these the etch rate of silicon decreases. But, the oxide etch rate is virtually unaffected since the number of impinging ions is unaltered[28].

The analysis presented in the above paragraph is applicable only when the pressure effect is studied at constant power level. However, in studies like the present one, the DC bias is maintained constant while the pressure variation is analyzed. This alters the power requirement from run to run

and hence, the number of ions is no longer a constant. At a constant bias, the average energy of the bombarding ions is a constant. As a consequence of the increase in the number of ions, as pressure increases, both silicon dioxide and silicon etch rates would increase due to the removal of polymer film by ion bombardment. In the case of silicon reduction in the number of neutrals may play an added role.

3.9.3. Effect of CHF_3 and CH_4:

As the CHF_3 flow rate increases, the oxide and Si etch rate drops due to enhanced polymerization[19]. The trend is similar for methane addition[17].

3.9.4. Effect of Oxygen:

Addition of O_2 increases the etch rates of Si by increasing the fluorine atom concentration and reducing the polymer deposition[9]. Etching of SiO_2 is largely unaffected by the addition of oxygen[28]. The selectivity for oxide etching is reduced by oxygen addition[20].

3.10. Justification for the Current Work

From the work reviewed above, it can be seen that SiO_2 etching selectivity and anisotropy can be improved under the following conditions:

i) Etching in RIE mode.

ii) Increase in C/F ratio.

iii) Addition of hydrogen containing species which would lead to HF formation and reduction in [F·].

iv) Additives that would facilitate polymer film formation.

CHF_3/CH_4 mixture satisfies all the above requirements in an RIE mode. Hence, it was expected to yield good selectivity. The results obtained confirmed the hypothesis.

In the RIE etching of SiO_2 by CHF_3/CH_4 mixture the reactor had to be cleaned after every use[17]. In some of the etching studies using CHF_3, it was reported that CHF_3 had to be mixed with an oxidant[16,19-21] in order to avoid polymerization and to achieve reproducible etching. O_2 addition is known to decrease polymerization. Hence, O_2 was added in our studies to CHF_3/CH_4 mixture.

4. EXPERIMENTAL PROCEDURE

The effect of addition of methane to trifluoromethane/oxygen mixture on the RIE etching of silicon dioxide and silicon was studied. Silicon wafers 4" in diameter were oxidized thermally and a pattern was etched on the oxide surface such that silicon was exposed in the etched regions. The wafers thus prepared were subjected to RIE etching in an AME-8110 etcher.

4.1. Wafer Preparation

4.1.1. Thermal Oxidation of Si Wafers:

A layer of thermal oxide 8000-9000 Å thick was grown on Si wafers in about 48 hours by atmospheric oxidation in a furnace at 1100-1200 ^{0}C.

4.1.2. Photolithographic Processing:

A resist pattern was developed on the oxidized wafer using the standard photolithographic sequence[29]. The wafer was coated with the positive photoresist S1400-27 by Shipley in the spinner at about 5000 RPM in 30 seconds. The resist was soft-baked in an oven at 90 ^{0}C for 30 minutes. After cooling, the wafers, covered with a mask containing the pattern shown in Figure 13, were exposed to UV light for about 1 minute.

The pattern was developed on the wafers by immersing the exposed wafer in the developer, AZ400K, for 1 minute. In this step, the exposed resist dissolves in the developer leaving a pattern of the unexposed resist on the wafer. Subsequently, the developer was washed away from the wafer by water rinse. The wafers were then dried by an air jet so that the wafer surface is spotless.

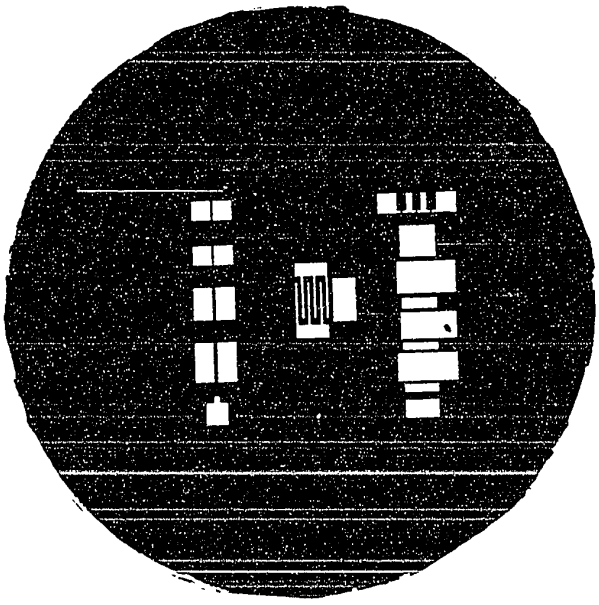

Figure 13. Pattern of Oxide over Silicon

4.1.3. Oxide Etch and Resist Stripping:

Buffered HF is known to etch silicon dioxide without destroying the resist integrity[30]. No report containing the silicon etch rates in buffered HF could be found in the literature. Since, in our studies, the Si etch rates were

determined by measuring the step in silicon, it was necessary to have a wafer with step free silicon surface or with a known step in silicon. Hence, the etch rate of silicon in buffered HF had to be determined. The etch rate of silicon in buffered HF was determined to be about 2-3 Å/min. The experimental procedure followed in the etch rate determination is described in Appendix 1.

The exposed oxide was removed by immersing in the buffered HF for about 8-9 minutes until all the oxide was etched away**. The wafer was then washed with water and dried in an air jet. Subsequently, the resist was stripped away by immersing for 3 minutes in a stripper bath of 10% p-toluene sulfonic acid by weight in DMSO maintained at 75^0C. This was followed by water wash and air jet drying of the wafer. Moisture was removed from the processed wafers by baking in an oven for 30 minutes at 100 ^{0}C. The above mentioned process sequence resulted in a pattern of oxide on silicon.

4.2. Plasma Etching

The wafers containing a pattern of silicon dioxide on silicon were dry etched in an AME-8110 RIE etcher. An

---

** Overetching the oxide for 1-2 minutes was not a concern since silicon etch rates were only about 2-3 Å/min and the experimental error in thickness measurements is 20-50 Å.

illustrative diagram of the AME-8110 hexode etcher is given in Figure 14. The etcher is a batch type reactor. The process chamber consists of a stainless steel bell jar that can be raised and lowered by a mechanical hoist assembly and a vertical, hexagonal RF cathode or hexode. The hexode, is mounted on an aluminum base plate. When the bell jar is lowered, it seals to the baseplate and encloses the hexode to form the process chamber. During processing, RF power (13.56 MHz) is applied to the hexode from the RF generator through a matching network and RF coupling device. The grounded base plate and bell jar together form the anode. The anode to cathode ratios about 2.5/1. This unsymmetrical electrode configuration leads to a high ion energy towards the substrate surface and low anode sputtering. The gas mixture is dispersed into the process chamber uniformly by means of the six stainless steel tubes installed on the inside of the bell jar. A combination of cryo and turbo pump systems is used to evacuate the chamber. Mass flow controllers control the gas flow. Pressure in the process chamber is monitored by a combination of thermocouple vacuum gauge, ion gauge and capacitance manometer. All the system functions are controlled by a microprocessor.

Temperature of the hexode is maintained at 25°C during etching. The etchings were performed under constant bias

mode for 10 minutes. The power required to maintain the bias was noted after 5 minutes of etch. By this time the plasma would have reached an equilibrium steady state and the power requirements remain constant. An upper power limit of 1800 W was set for the safety of the reactor. The etcher is reported to etch with a variation of < 5% in thickness across the wafer.

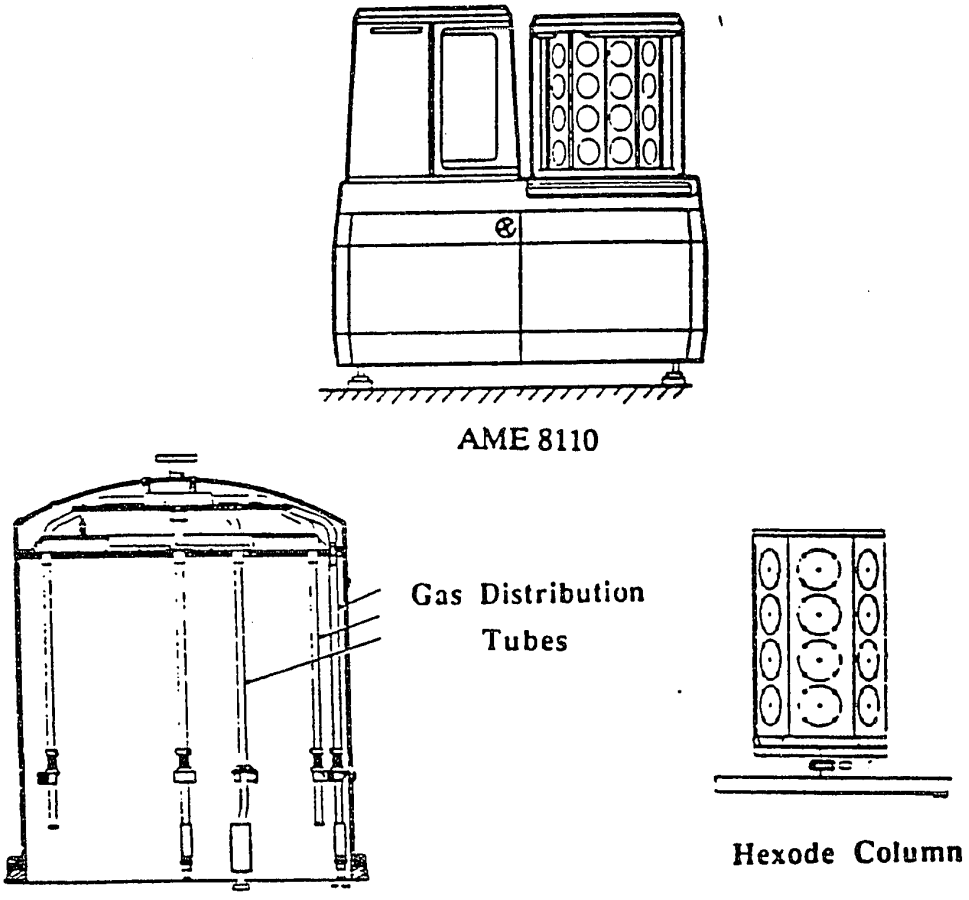

Figure 14. Schematic Diagram of an AME-8110 RIE System

4.3. Measurement of Oxide Etch Rate

SiO_2 etch rates were measured using a NanoSpec micro area gauge by measuring the oxide thickness prior to (t_i) and following (t_f) each run. The thickness of the oxide layer was the average of six measurements, four of which were close to the edges and two were at the center. The etch rate was calculated by dividing the difference between the oxide thicknesses before and after the etch, i.e., (t_f - t_i), by the time, namely, 10 minutes. Minimum thickness that can be measured using the NanoSpec is 100 Å.

4.4. Measurement of Silicon Etch Rate

After the determination of oxide thickness, the oxide layer was etched to about 1000 Å in dilute HF*. The etch rate of SiO_2 in dilute HF is about 150-200 Å/minute[30]. After dilute HF etch, the oxide thickness (t_e) was measured using the NanoSpec. The step in the wafer along the pattern (t_s) was then measured using an Alpha Step Profiler. The step is the resultant of oxide film and etched silicon. Amount of silicon etched was obtained by subtracting the oxide thickness measured using the NanoSpec after dilute HF etch from the step measured using the Alpha Step Profiler. Silicon etch rate is amount of silicon etched divided by the

*An oxide layer was found to be necessary in order to make the pattern visible while measuring the step.

etch time, namely, 10 minutes ((t_s -t_e)/10). Control measurements done to calibrate the two instruments, i. e., the NanoSpec and Alpha Step Profiler, with respect to one another gave thickness values differing within 20-30 Å for an oxide film of thickness about 1000 Å.

4.5. Variable Ranges

This study was intended to determine the effect of variables using Response Surface Methodology[31] discussed in Appendix 2 in the ranges given in Table 2. These initial ranges for the process variables were chosen within the limits of the etcher capabilities from the literature reports on related processes.

Preliminary experiments were conducted within the ranges given in Table 2 to choose the range settings for the first order fit. These ranges are given in Table 3. The design of experiments, chronology of data collection, and first and second order data analyses are discussed in detail in Appendix 2. Fractional factorial design was used to generate the 19 experimental conditions for the first order fit. Since the fit obtained from the first order analysis was poor, six additional experiments were conducted within or close to the ranges given in Table 3 to fit a second degree polynomial. The range settings provided in Table 3

is considered as the narrow range in our studies.

The ranges of the variables given in Table 3 represent a narrow region of the reaction surface that was intended to be explored. However, as will be seen in detail in Appendix 2, design of experiments techniques could not be used in further exploration the reaction surface. Experiments were performed at random in the expanded reaction surface described in Table 4. These ranges were narrower than the originally intended ones due to the process characteristics.

Table 2. Variables and their Initial Ranges

Variable	Variable Name	Range
DC Bias	X1	-300 - -900 V
Pressure	X2	10 - 100 mT
CHF_3 Flow Rate	X3	50 - 100 sccm
CH_4 Flow Rate	X4	0 - 10 sccm
O_2 Flow Rate	X5	0 - 10 sccm

Table 3. Narrow Variable Ranges

Variable	Variable Name	Range
DC Bias	X1	-600 - -700 V
Pressure	X2	30 - 50 mT
CHF_3 Flow Rate	X3	50 - 100 sccm
CH_4 Flow Rate	X4	0 - 6 sccm
O_2 Flow Rate	X5	9 - 15 sccm

4.6. Regression Analysis

A total of 53 experiments were performed. In some runs polymer formation on the wafer surface or nonuniformity in etching prevented the determination of etch rates. The data obtained from the rest of the runs were analyzed by regression methods using the computer program XSTAT[32]. XSTAT is capable of designing experiments and analyzing the data. Data not conforming to any design of experiments technique could also be analyzed using XSTAT.

Table 4. Expanded Reaction Surface

Variable	Variable Name	Range
DC Bias	X1	-500 - -800 V
Pressure	X2	20 - 50 mT
CHF_3 Flow Rate	X3	50 - 100 sccm
CH_4 Flow Rate	X4	0 -8 sccm
O_2 Flow Rate	X5	5 - 15 sccm

Since first order regression analysis of the data suggested lack of fit, second order regression equations were used. Two sets of second order regression equations were obtained; one in the narrow range (Table 3) with 25 data points and the other in the expanded range (Table 4) with 42 points. Since the fit was poor for selectivity in the expanded range, the regression equation for the narrow range was used to generate the plots illustrating the effects of variables.

4.7. Change in Power Requirements

There was a time delay of about two weeks between the experiments conducted in the narrow range and the expanded range. For an unknown reason, a jump in power requirements was noticed while conducting the additional experiments in the expanded reaction surface. The etch rates were observed to be higher in these experiments. Hence, the data collected for the additional 17 runs in the expanded surface was corrected. It has to be noted that similar power variations were observed by other experimenters on this equipment in our laboratories. However, no variation in etch rates were noticed in those studies.

The correction factor was calculated from the experiments conducted under the same reaction conditions prior to and after the occurrence of the power jump. The calculation of the correction factor is discussed in Appendix 2.

5. RESULTS

The etch rates and selectivities were fitted with a second degree polynomial using XSTAT. The data were fit in the two ranges, i.e., the narrow and expanded range. The R-squared term was used to estimate the closeness of the fit. The salient features of the results obtained are summarized in the section 6.3.

5.1. Second Order Analysis in the Narrow Range

The data obtained from the first 26 experiments is used for the second order analysis in the narrow range described in Table 3. These data given in Table 5, are fitted using XSTAT with the second degree polynomial given below.

$$Y = b_0 + \Sigma\, b_i X_i + \Sigma\,\Sigma\, b_{ij} X_i X_j + \Sigma\, b_{ii} X_i^2$$

All three responses, namely, the two etch rates and the selectivity were analyzed by the least squares regression method. The results obtained for the second order model is presented in Table 6.

All three responses are represented very well by the second order model as indicated by a high R-squared value. The fit improves from 95.3% to 99.1% if log(selectivity) is used as the response instead of selectivity.

Table 5. Etch Rates and Selectivities for the Second Order Fit in the Narrow Range

No.	Run No.	X1, -V	X2, mT	X3, sccm	X4, sccm	X5, sccm	Y1, Å/mi	Y2, Å/mi	Y3
1	13	600	30	50	0	15	318	246	1.29
2	5	600	30	50	6	9	342	18	19.00
3	10	600	30	100	0	9	423	55	7.69
4	2	600	30	100	6	15	400	40	10.00
5	16	600	50	50	0	9	540	110	4.91
6	4	600	50	50	6	15	491	76	6.46
7	11	600	50	100	0	15	608	127	4.79
8	19	600	50	100	6	9	336	21	16.00
9	7	700	30	50	0	9	489	121	4.04
10	14	700	30	50	6	15	435	72	6.04
11	3	700	30	100	0	15	552	104	5.31
12	17	700	30	100	6	9	462	30	15.40
13	9	700	50	50	0	15	650	178	3.65
14	8	700	50	50	6	9	567	71	7.99
15	15	700	50	100	0	9	670	91	7.36
16	1	700	50	100	6	15	649	82	7.91
17	6	650	40	75	3	12	547	94	5.82
18	12	650	40	75	3	12	552	91	6.07
19	18	650	40	75	3	12	532	84	6.33
20	20	637	37	89	7	10	441	25	17.60
21	22	710	40	75	3	12	658	152	4.23
22	23	640	40	75	3	12	515	82	6.28
23	24	600	30	85	6	9	361	15	24.10
24	25	600	30	80	8	12	420	40	10.50
25	26	700	30	85	6	9	562	63	8.76

Table 6. Second Order Regression Analysis in the Narrow Range

Response	Variation, R-Squared
Y1, SiO_2 Etch Rate	99.58%
Y2, Si Etch Rate	99.80%
Y3, Selectivity	95.28%
Y4, log(Y3)	99.14%

5.2. Second Order Analysis in the Expanded Surface

The data provided in Tables 5 were analyzed together with the data collected in the expanded region using a second degree polynomial. The regression fit factor , R-squared, obtained from the analysis for all the three responses are tabulated in Table 7. The data in the expanded surface utilized in the analysis and not provided in Table 5 is given in Table 8.

Table 7. Second Order Regression Fit of Expanded Reaction Surface

Response	Variation, R-Squared
Y1, SiO_2 Etch Rate	97.77%
Y2, Si Etch Rate	95.98%
Y3, Selectivity	84.08%
Y4, log(Y3)	93.91%

It can be seen from Table 7 that the fit for selectivity is poor in the expanded range. Though the R-square terms are lower for the etch rates also they are quite good (>95%).

Table 8. Additional Data in the Expanded Surface used in Second Order Fit

No.	Run No.	X1, -V	X2, mT	X3, sccm	X4, sccm	X5, sccm	Y1, Å/mi	Y2, Å/mi	Y3
1	27	575	45	75	0	8	459	71	6.46
2	28	575	45	75	0	8	459	67	6.90
3	29	650	40	75	3	12	550	90	6.11
4	30	575	45	75	3	8	369	43	8.58
5	31	575	45	75	5	8	266	19	14.00
6	32	575	35	75	3	5	319	24	13.30
7	33	575	45	75	3	5	330	36	9.17
8	34	575	45	75	0	5	465	60	7.75
9	35	750	20	50	6	9	385	30	12.90
10	36	650	40	75	3	12	540	85	6.21
11	38	800	20	50	6	9	458	38	12.10
12	39	550	35	50	6	9	302	15	20.10
13	40	550	20	50	6	9	178	22	8.09
14	41	650	20	50	6	9	246	18	13.70
15	42	500	30	75	3	8	232	29	8.00
16	43	750	30	100	6	9	549	41	13.40
17	44	550	40	91	1	5	356	77	4.62

5.3. Summary

The overall trends in etch rates and selectivity are summarized in Section 6.3. The salient features of the results obtained are:

i) Both oxide and Si etch rates increase with increases in bias and pressure.

ii) Both oxide and Si etch rates decrease with the

addition of methane. The Si etch rate decreases more drastically relative to the oxide etch rate leading to an increase in selectivity. For example, in the experiments conducted at -575 V bias, 45 mT pressure, 75 sccm CHF_3 flow rate, and 8 sccm O_2 flow rate, 5 sccm of methane flow rate decreased the silicon etch rate by as much as 65% while the oxide etch rate dropped only 28%.

iii) The trends observed are consistent with the trends expected from the literature review and presented in Section 3.9.

iv) The maximum selectivity obtained was 24.

6. DISCUSSION

The regression equations obtained from second order analyses were used to generate the plots illustrating the effects of variables. Since the fit obtained for selectivity in the expanded surface was poor, the regression equation obtained in the narrow range (Table 3) is used for generating the plots for selectivity. For the plots of oxide and silicon etch rates the regression equation obtained in the expanded surface were used.

6.1. Selectivity

It can be seen from Table 7 that the experimental data could be fit quite well by the second order model for SiO_2 and Si etch rates in the expanded surface. However, selectivity can not be adequately expressed in terms of the second degree polynomial in the expanded reaction surface. Though the fit improves when log(selectivity) is used, the high value of F-ratio (31.4) suggests that the regression equation is not reliable enough for predicting the optimum.

Since it was not possible to predict the conditions of maximum selectivity using the model, the maximum was picked up from the available data points. The maximum in selectivity was 24 and the corresponding conditions were:

Bias	=	-600 V
Pressure	=	30 mT
CHF_3 Flow Rate	=	85 sccm
CH_4 Flow Rate	=	6 sccm
O_2 Flow Rate	=	9 sccm

Experiments done under the standard conditions suggested by the instrument manufacturer (Bias = -575 V, Pressure = 45 mT, CHF_3 Flow = 75 sccm, and O_2 Flow = 8 sccm) with and without methane flow showed that methane addition does increase the selectivity in oxide etching. The results of these experiments are presented in Table 9.

Since the fit for selectivity was poor in the expanded surface, plots of the effects of variables could not be obtained in this range. However, the R-Squared term (95.28%) obtained from the data in the narrower range (Table 3) indicates a reasonable fit. Hence, the plots presented in Figures 15-19 are created from the regression equation for the narrow range. The regression equation is:

$$Y3 = 92.61 + 0.01306*X1 + 3.799*X2 - 0.3184*X3 + 10.35*X4 - 26.62*X5 + 0.000951*X1*X2 + 0.000184*X1*X3 - 0.009406*X1*X4 + 0.008281*X1*X5 + 0.001033*X2*X3 - 0.03025*X2*X4 + 0.02080*X2*X5 - 0.001242*X3*X4 - 0.000015*X3*X5 - 0.1383*X4*X5 - 0.000124*X1^2 - 0.059*X2^2 + 0.001411*X3^2 - 0.03895*X4^2 + 0.8353*X5^2$$

Table 9. Effect of Methane Addition

Run No.	CH_4 Flow Rate, sccm	SiO_2 Etch Rate, Å/min.	Si Etch Rate, Å/min.	Selectivity
27	0	514	72	7.14
30	3	474	51	9.29
31	5	370	25	14.80

Figures 15-19 show that increases in bias and O_2 flow rate decrease the selectivity while increases in CHF_3 and CH_4 flow rates increase the selectivity. Experimental data indicates a maximum in selectivity around -600 V. Increase in pressure leads to a maximum in selectivity around 35 mT. These effects, discussed in Section 6.3, agree quite well with the reported trends presented in Section 3.9.

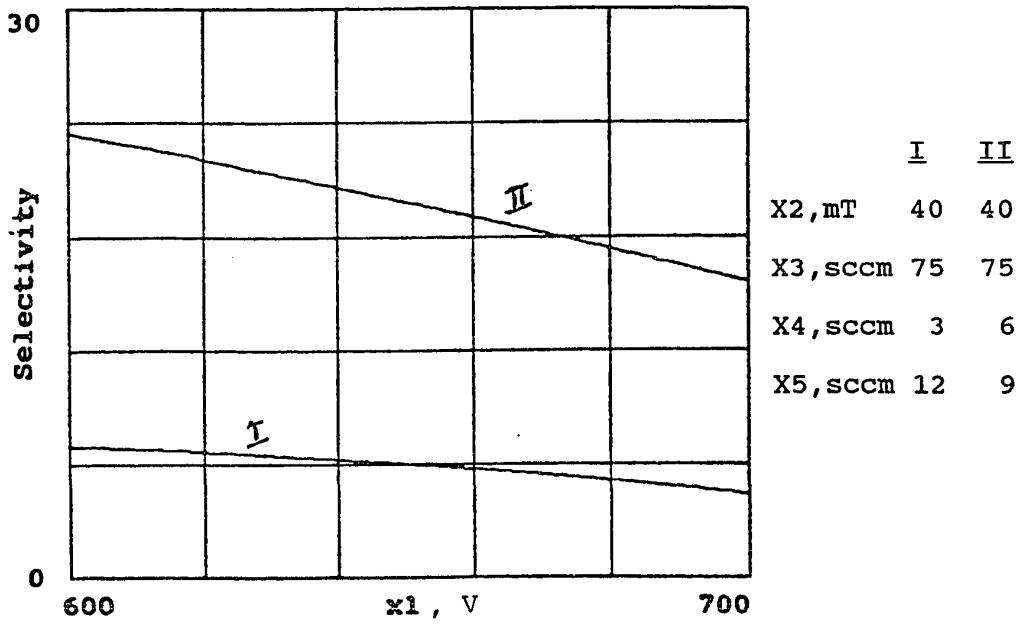

Figure 15. Effect of Negative Bias, X1, on Selectivity

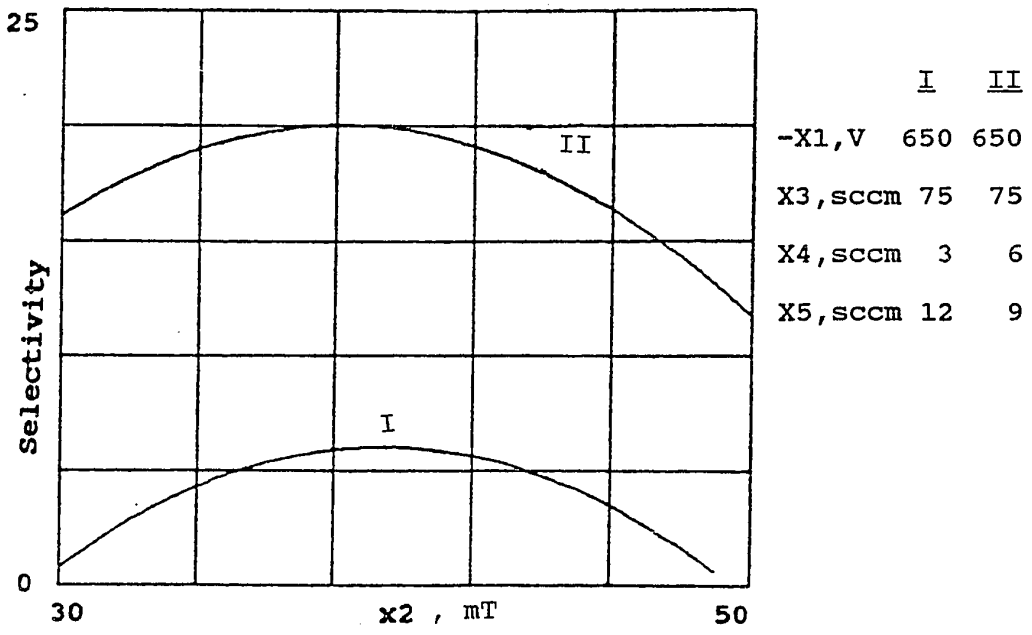

Figure 16. Effect of Pressure, X2, on Selectivity

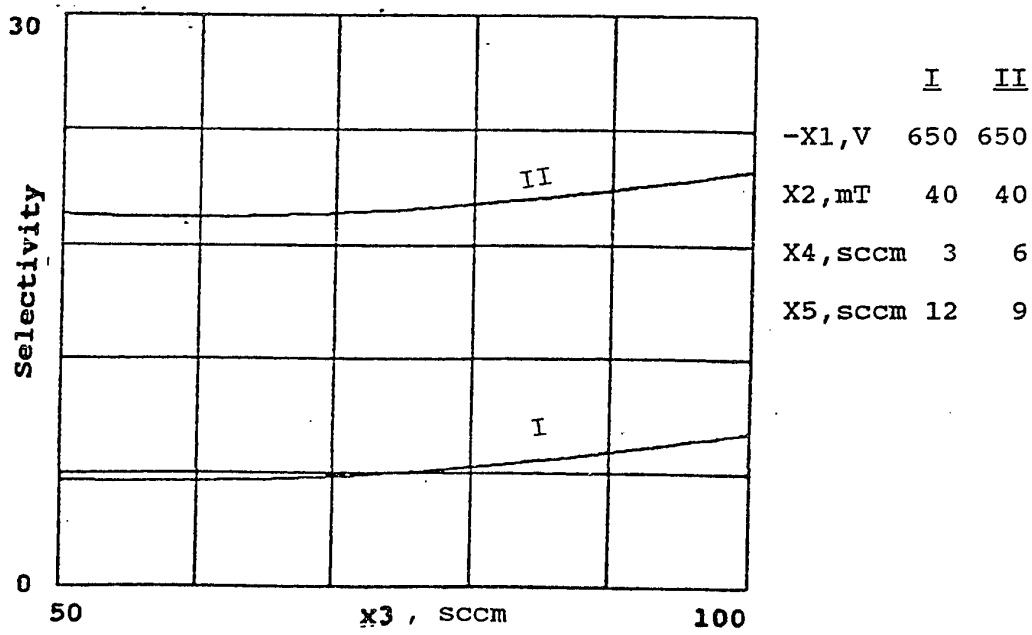

Figure 17. Effect of CHF_3 Flow Rate, X3, on Selectivity

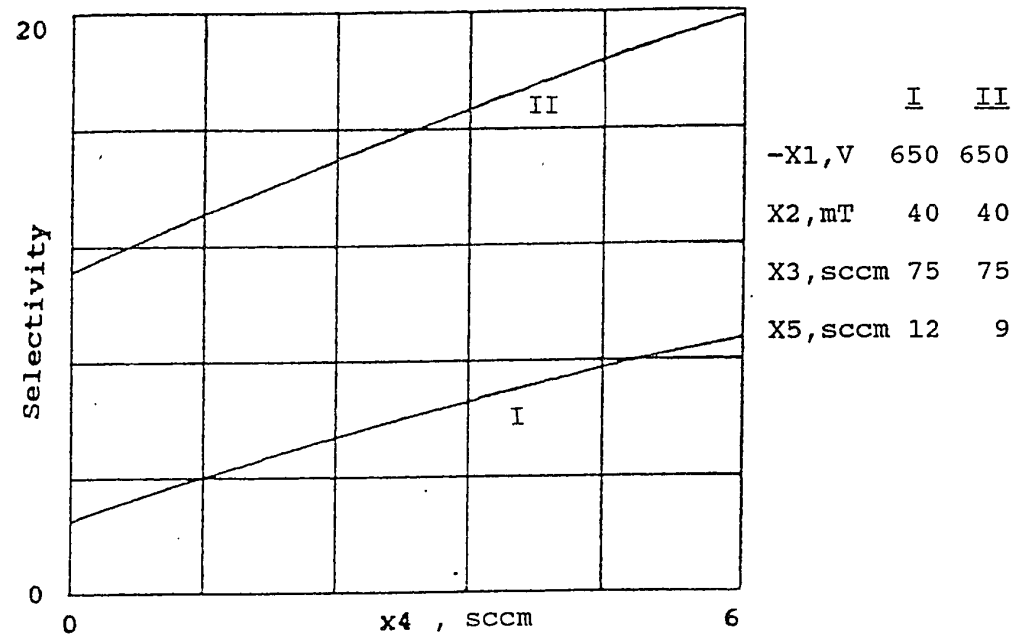

Figure 18. Effect of CH_4 Flow Rate, X4, on Selectivity

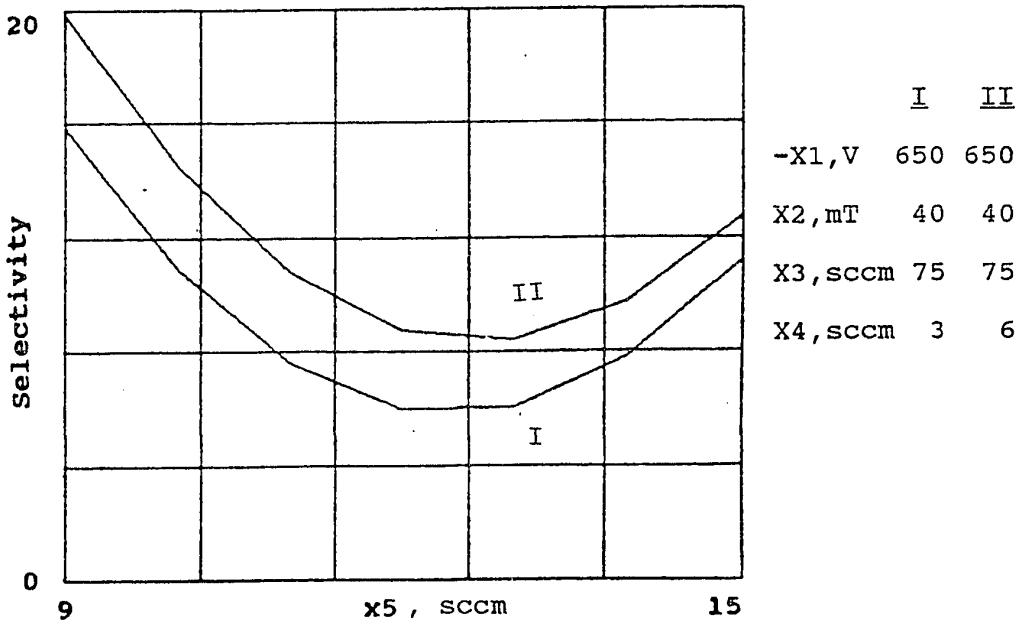

Figure 19. Effect of O_2 Flow Rate, X5, on Selectivity

6.2. SiO_2 and Si etch Rates

The regression analysis of SiO_2 and Si etch rates indicated good fit for the data using the second order equation (Table 15). Hence the effect of the experimental variables were analyzed using the regression equations. The regression equations are:

$$
\begin{aligned}
Y1 = & -175.4 - 0.6944*X1 + 5.515*X2 + 3.065*X3 - 31.95*X4 \\
& + 10.35*X5 + 0.03275*X1*X2 + 0.008151*X1*X3 + \\
& 0.02623*X1*X4 - 0.08551*X1*X5 - 0.04091*X2*X3 - \\
& 0.6915*X2*X4 + 0.7108*X2*X5 - 0.2173*X3*X4 + \\
& 0.2828*X3*X5 + 2.570*X4*X5 + 0.000984*X1^2 - \\
& 0.2898*X2^2 - 0.05697*X3^2 + 2.686*X4^2 - 0.2360*X5^2
\end{aligned}
$$

$$
\begin{aligned}
Y2 = & \ 319.3 - 0.9725*X1 - 13.24*X2 - 0.9138*X3 - 48.45*X4 \\
& + 53.70*X5 + 0.01973*X1*X2 + 0.004089*X1*X3 + \\
& 0.03572*X1*X4 - 0.07926*X1*X5 + 0.03572*X2*X3 + \\
& 0.2113*X2*X4 - 0.1729*X2*X5 + 0.1588*X3*X4 - \\
& 0.07570*X3*X5 - 0.9754*X4*X5 + 0.000702*X1^2 - \\
& 0.03298*X2^2 - 0.03598*X3^2 + 1.028*X4^2 + 0.9202*X5^2
\end{aligned}
$$

Using these regression equations plots of etch rates given in Figures 20-29 were constructed as a function of the variables.

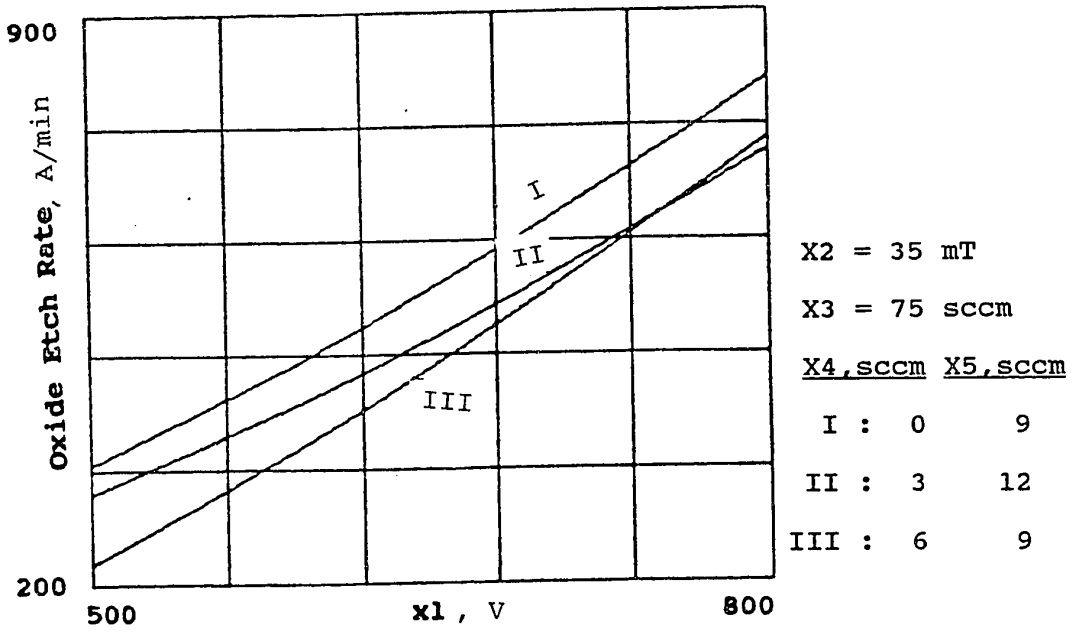

Figure 20. Effect of Negative Bias, X1, on the Oxide Etch Rate

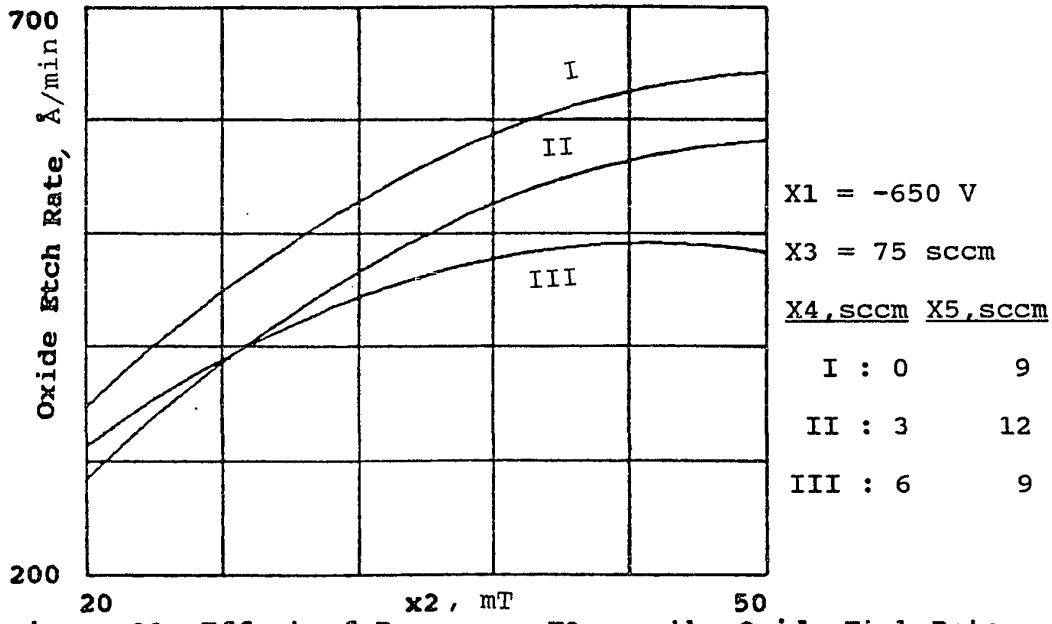

Figure 21. Effect of Pressure, X2, on the Oxide Etch Rate

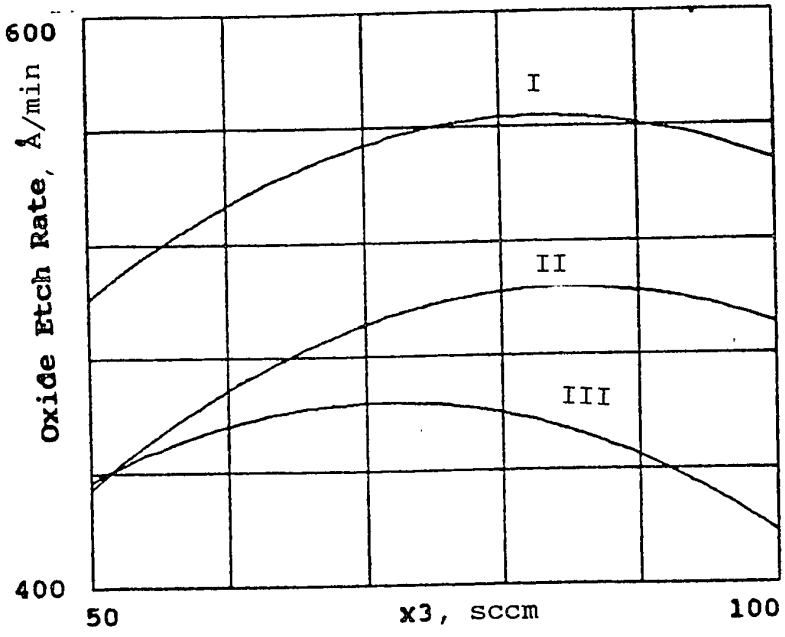

X1 = -650 V

X2 = 40 mT

	X4, sccm	X5, sccm
I :	0	9
II :	3	12
III :	6	9

Figure 22. Effect of CHF_3 Flow, X3, on the Oxide Etch Rate

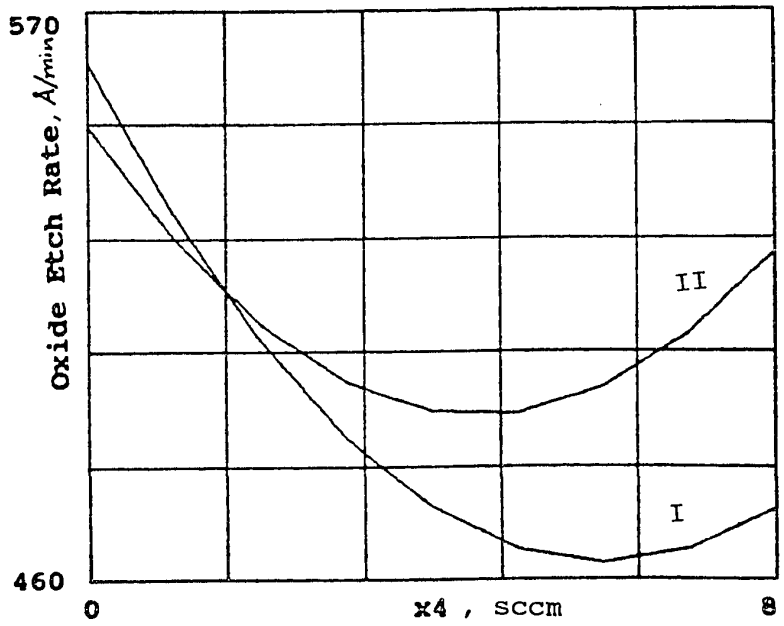

X1 = -650 V

X2 = 40 mT

X3 = 75 sccm

X5 =

I: 9 sccm

II: 12 sccm

Figure 23. Effect of CH_4 Flow, X4 (sccm), on the Oxide Etch Rate

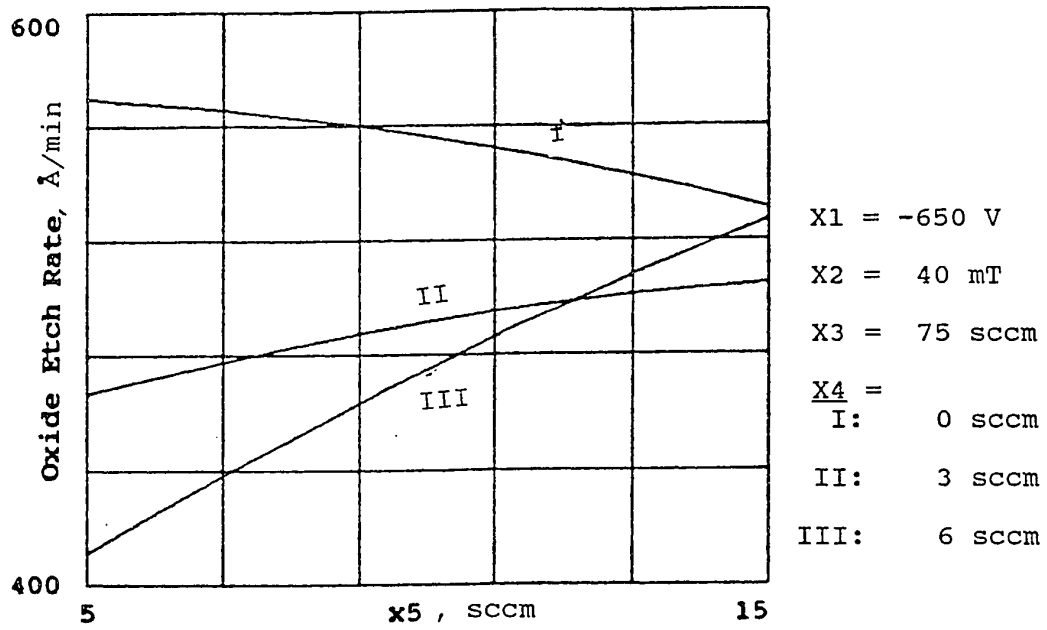

Figure 24. Effect of O_2 Flow, X5 (sccm), on the Oxide Etch Rate

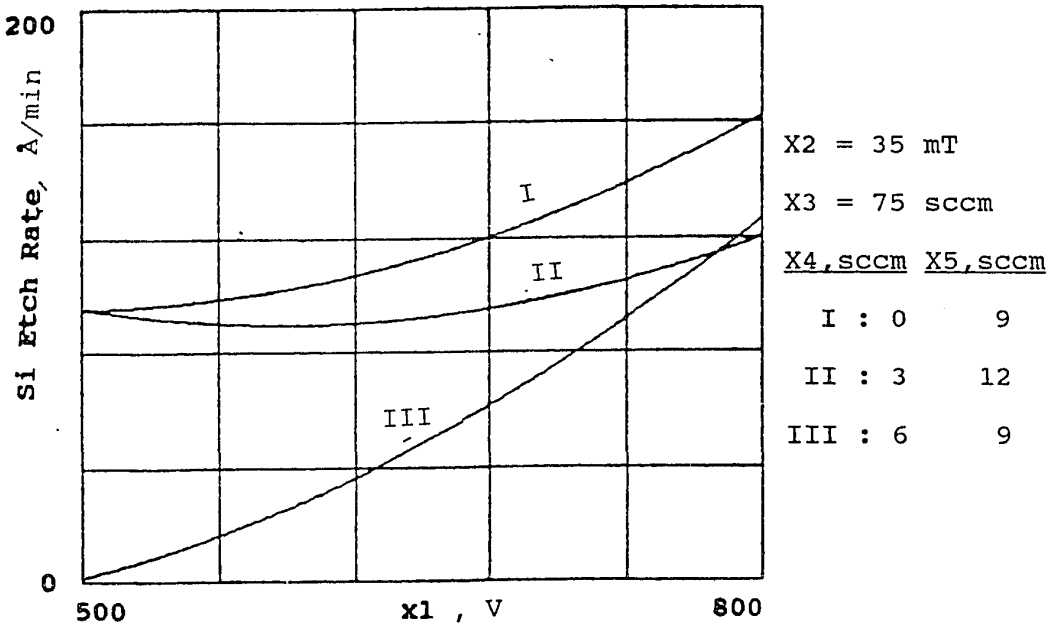

Figure 25. Effect of Negative Bias, X1, on the Si Etch Rate

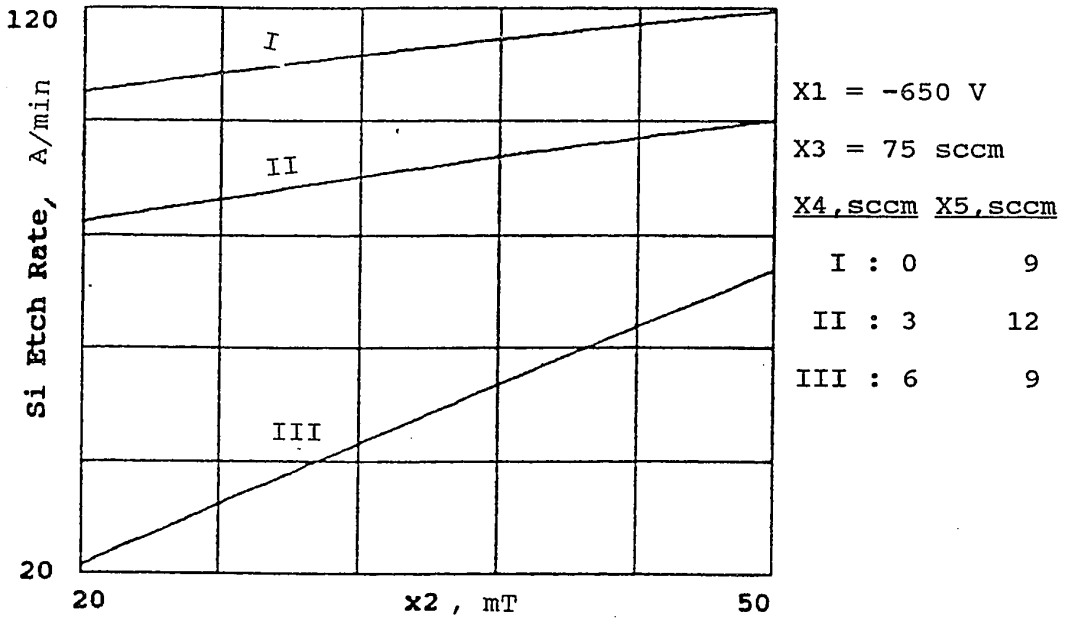

Figure 26. Effect of Pressure, X2, on the Si Etch Rate

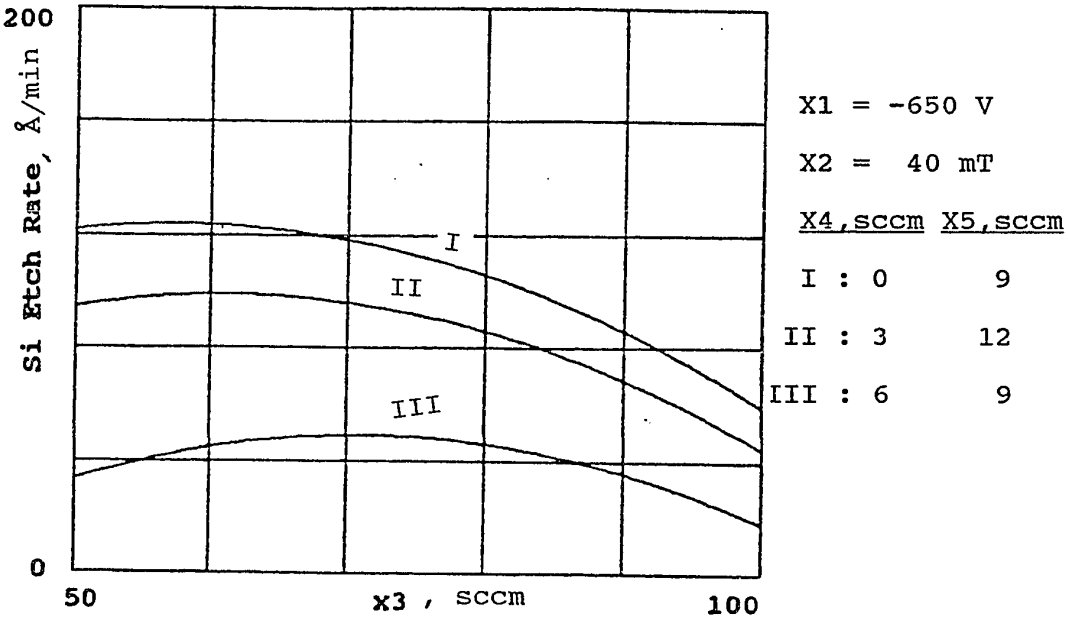

Figure 27. Effect of CHF_3 Flow, X3, on the Si Etch Rate

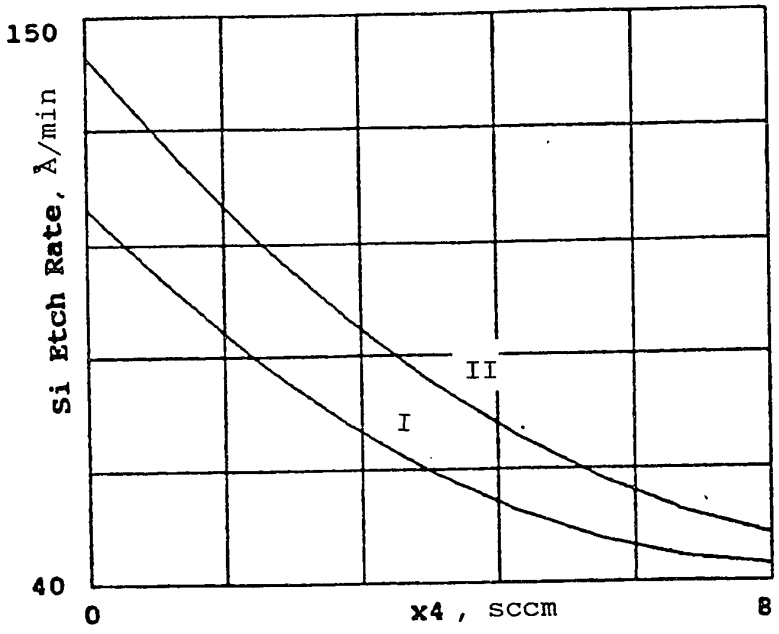

Figure 28. Effect of CH_4 Flow, X4 (sccm), on the Si Etch Rate

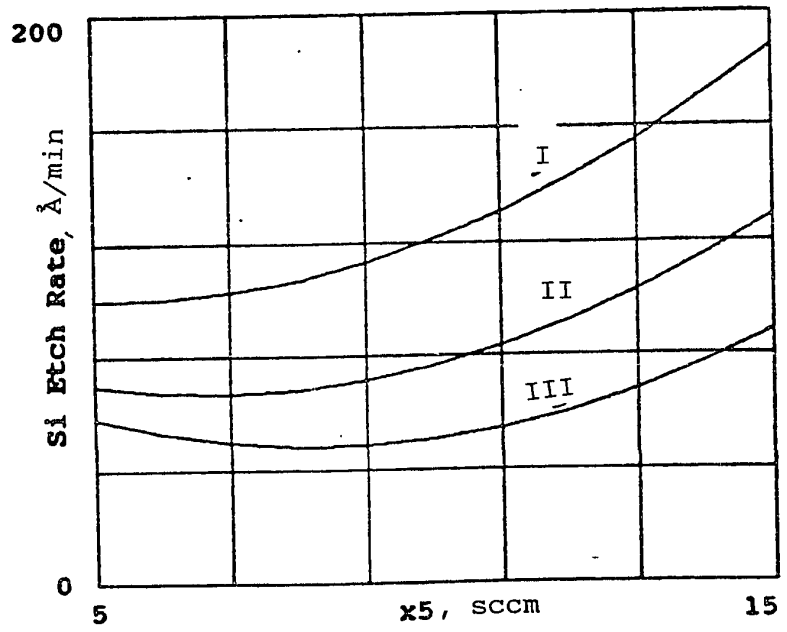

Figure 29. Effect of O_2 Flow, X5 (sccm), on the Si Etch Rate

The influence of the variable parameters are summarized in Section 6.3. These trends are consistent with the expectations based on the mechanism of etching discussed in Section 3.9. The variations in the Si and SiO_2 etch rates are related to the fluorine atom concentration, polymer film formation and removal, HF formation, and ion bombardment.

6.3. Influence of Variables

The effects of variables on the etch rates and selectivity are summarized in Table 10. The plots generated using the regression equations (Figures 15-29) were used to generate this table.

Table 10. Influence of Variables

Variable	SiO_2 Etch Rate	Si Etch Rate	Selectivity*
DC Bias ↑	↑	↑	↑@ then ↓
Pressure ↑	Asymptotic ↑	↑	↑ then ↓
CHF_3 ↑	↑ then ↓	↑ then ↓	↑
CH_4 ↑	↓ then ↑	↓	↑
O_2 ↑	↓ (No CH_4)	↑	↓ then ↑
	↑ (CH_4)		

* - Trends noted from narrow range plots can be extrapolated to the expanded surface.
@ - Experimental data in the region -500 to -600 V show an increase in selectivity in this region. Rate is not available.)

An increase in bias leads to an increase in both the etch rates. Oxide etch rate varies almost linearly at a rate of

about 1.5 Å/min/V whereas the increase in Si etch rate becomes significant at bias levels over -600 V. Ion bombardment is the cause of increased etch rates[5]. There is a maximum in selectivity around -600 V. The increase in selectivity with bias in the range -500 to -600 V followed by a decrease beyond -600 V can be explained on the basis of the variation in slope in the silicon etch rate versus bias curve (Fig. 25). At lower biases, physical sputtering of polymeric layer formed on Si may not be high enough to effect a significant increase in silicon etching. The selectivity increases under these conditions since the rate of increase in Si etch rates is not high enough to match the rate of increase in oxide etch rate. At bias values higher than -600 V, the increase in etch rate with bias is more pronounced for silicon etching in comparison with oxide etching, and hence the selectivity decreases with increase in bias. For example, at a pressure of 35 mT, and flow rates of 75, 6, and 9 sccms of CHF_3, CH_4, and O_2, the Si etch rate increases at a rate of 0.25 Å/min/V in -500 to -600 V region, while it increases at a rate of about 0.45 Å/min/V in the range -600 to -700 V. This difference in the rate of increase in Si etch rate is responsible for the drop in selectivity beyond -600 V following initial increase.

The effect of pressure is quite complex. Free radical

concentrations decrease and the number of bombarding ions increases with pressure at a constant bias (see Section 3.9 for details). With an increase in pressure, there will be a decrease not only in the fluorine atom concentration but also in the thickness of the in situ polymer film. These effects lead to an asymptotic increase in oxide etch rates (Fig. 21) and a steady increase in silicon etch rates (Fig. 26) under the experimental ranges studied. Due to the asymptotic nature of the pressure effect on oxide etch rate, the increase in oxide etch rate is not high enough to sustain an increase in selectivity at pressures over 35 mT. Hence, there is a maximum in the selectivity versus pressure curves (Fig. 16). For example, at a bias of -650 V, and CHF_3, CH_4, and O_2 flow rates 75, 6, and 9 sccm, the oxide etch rate increases from 320 Å/min. at 20 mT pressure to 470 Å/min. at 35 mT, and 490 Å/min. at 50 mT. This translates to about 2.5% increase per mT in oxide etch rate in the first half of the pressure range while in the second half the increase is only about 0.27% per mT. Under the same conditions of bias and flow rates, the silicon etch rate increases quite steadily from 25 Å/min. to 75 Å/min. giving a rate of increase of 3.3% per mT in the entire range. The variation in slope in the pressure effect curve of the oxide etch rate around 35 mT coincides roughly with the occurrence of a maximum in the selectivity curve (Curve II, Fig. 16).

Both fluorine atom and CF_x radical concentrations will increase with an increase in CHF_3 flow rate. Initially, both the etch rates increase with CHF_3 flow (Figs. 22 and 27). As the CHF_3 flow rate increases beyond about 75 sccm, the etch rates decrease probably due to increased polymerization. Since both the etch rates follow the same pattern, the effect of CHF_3 flow rate on selectivity is quite small (Fig. 17).

Methane addition decreases both the etch rates (Figs. 23 and 28) due to increased polymerization[17]. The increase in oxide etch rate beyond 6 sccm of CH_4 flow (Fig. 23) can not be explained. The decrease in etch rate is more significant for silicon. This is probably due to the fact that fluorine atom concentration is significantly reduced by HF formation, and that no other species is available to etch silicon. However, the reaction of oxide with the CF_x film will result in oxide etching. These two factors together are responsible for the increase in selectivity observed by the addition of methane. Though in theory an infinite selectivity can be achieved by adding methane, the optimum amount of methane that can be added is only about 8%. This is due to the drop in oxide etch rate and increased polymerization which makes the process economically not viable.

The concentration of fluorine atoms increases with increase in oxygen content[9]. This causes the observed increase in Si etch rate (Fig. 29). However, up to about 3 sccm of oxygen flow, oxygen addition has little effect on silicon etch rates even in the absence of methane. Removal of the polymer film deposited on Si would consume some oxygen and the reduction in thickness of the film may be crucial in the etching of silicon by fluorine radicals produced by the reaction of CF_x with O_2. Oxide etch rate decreases with oxygen content in the absence of methane and increases in the presence of methane (Fig. 24). In the absence of methane, oxygen reacts with CF_x radicals/film, thereby competing with oxide etching and resulting in reduced oxide etch rates. The observed increase in oxide etch rate with oxygen addition in the presence of methane, can be explained by the possible competition for oxygen from the radicals or film originating from CH_4 with CF_x species. This competition would make the CF_x available for oxide etching. The selectivity decreases with an increase in oxygen flow rate in accordance with the literature reports[20]. This trend is only up to 12 sccm of oxygen flow. Beyond this flow rate the selectivity increases (Fig. 19) for which no explanation could be given. Though the selectivity decreases with oxygen addition, oxygen was found to be necessary for the etching to proceed without inhibition by

polymerization on the wafers. The required oxygen content increases with increase in methane concentration.

The highest value of selectivity obtained from the available data correspond to -600 V of bias, 30 mT pressure, 85, 6, and 9 sccm of CHF_3, CH_4, and O_2 respectively. Under these conditions the oxide and Si etch rates were 361 and 15 Å/min. respectively and the selectivity was 24. These conditions are quite close to the conditions of maximum in the selectivity versus bias and pressure curves, i. e., -600 V and 35 mT. As seen in the above paragraphs, CHF_3 flow rate has a very small effect on selectivity (less than 3 units for a variation of 50 sccm). The upper limit on the methane flow is about 8% and corresponds to the polymer point. Beyond this limit polymerization leads to significant reductions in the etch rates and reproducibility. A minimum of about 10% of oxygen is required in the presence of methane in order to minimize the adverse effects of polymerization.

6.4. Reliability of the Observed Trends

The plots describing the effects of the variables were obtained using the second degree polynomials obtained from the regression analysis of the data. The overall trends observed in these plots fit quite well with the expectations

based on the available reports. However, there are some discrepancies that can not be explained. Some of these are:

i) Increase in oxide etch rate with increase in CH_4 flow beyond 6 sccm observed in Figure 23.

ii) Zero or negative values of selectivity observed in Figure 16 between 48-50 mT pressure under conditions I.

iii) Increase in selectivity with increase in oxygen flow beyond 12 sccm as noted in Figure 19.

The analysis of F-ratio, that is the ratio of the lack of fit mean square to the replicate error can be used to find out if the lack of fit is caused by experimental error or not[35]. If the design includes replication, the residual mean square can be split into its lack of fit and replicate components. A large F-ratio would indicate that the residual is primarily caused by lack of fit rather than experimental error. The F-ratios observed in the regression analysis are presented in Table 11.

The high F-ratios obtained for all the three responses indicate that lack of fit is the primary cause of the residuals and not the experimental errors. The fit may be improved by using a higher order polynomial such as a cubic one. The polynomials used in regression analysis fit the available data. However, the actual etching process

involves a combination of several mechanisms. The mechanism of etching is oversimplified by these polynomials. Physical significance of the data should be combined with the analysis of the observed trends using these polynomials.

Table 11. F-Ratios of the Regression Analysis of The Etch Rates and Selectivity

Response	Lack of Fit Mean Square	Pure Error Mean Square	F-Ratio
Y1*	899.11	54.66	16.45
Y2*	246.40	18.00	13.69
Y3*	10.422	0.05857	177.93
log(Y3)*	0.009105	0.000290	31.37
Y3-NS#	17.169	0.08292	207.055

* - Expanded Reaction Surface; # - Narrow Surface

6.5. Summary

The overall trends obtained for the etch rates and selectivity conform to the expectations discussed in Section 3.9. The regression equations obtained from the analysis using XSTAT are used in the generation of plots presented in this Chapter. Though the second order polynomial gives a reasonably good fit as indicated by high R-Squared values reported in the previous Chapter, the analysis of lack of fit data indicates the necessity of a higher order model in fitting the data.

CONCLUSIONS

Second degree polynomials were fit by the regression analysis of the etch rates of silicon dioxide and silicon. The observed trends agreed quite well with the expectations based on the known mechanism. The addition of methane to CHF_3/O_2 feed gas mixture led to decrease in both oxide and silicon etch rates. Due to the steeper drop in the etch rate of silicon relative to oxide, an increase was observed in the selectivity in oxide etching. The maximum selectivity obtained for the oxide etching relative to silicon was 24.

REFERENCES

1. "VLSI Technology," edited by S.M. Sze, 2nd Edition, Mcgraw-Hill Book Company, New York, 1988.

2. "Plasma Etching in Semiconductor Fabrication," by Russ A. Morgan, Elsevier Publishers, 1985.

3. T. P. Chow, and A. J. Steckl, J. Electrochem. Soc., 131, 2325, (1984).

4. D. B. Graves, AIChE Journal, 35, 1, (1989).

5. "Plasma Etching - An Introduction," edited by D. M. Manos, and D. L. Flamm, Academic Press, San Diego, CA, 1989.

6. "Dry Etching for VLSI," by A. J. van Roosamalen, J. A. G. Baggerman, and S. J. H. Brader, Plenum Press, New York, 1991.

7. W. G. M. van den Hoek, C. A. M. de Vries, and M. G. J. Heijman, J. Vac. Sci. Technol., A1, 1795 (1983).

8. "Characterization of an AME-8110 Hexode Plasma Etcher," by M. Khan, a Report Submitted to the Department of General Engineering, San Jose State University, San Jose, 1992.

9. C. J. Mogab, A. C. Adams, and D. L. Flamm, J. Appl. Phys., 49, 3796, (1978).

10. R. A. H. Heinecke, Solid State Electronics, 18, 1146, (1975).

11. L. M. Ephrath, J. Electrochem. Soc., 126, 1419, (1979).

12. R. A. H. Heinecke, Solid State Electronics, 19, 1039, (1976).

13. B. A. Heath, J. Electrochem. Soc., 129, 396, (1982).

14. R. W. Light, and F. C. See, J. Electrochem. Soc., 129, 1152, (1982).

15. "Characterization of an AME-8110," by M. S. Kwan, a Report Submitted to the Center of Electronic Materials and Devices, San Jose State university, San Jose, 1991).

16. X.F. Meng, R.S. Amos, A.W. Lichtenberger, R.J. Mattauch,

and M.J. Feldman, IEEE Trans. Magn., 25, 1239, (1989).

17. H. Norstrom, R. Buchta, F. Runovc, and P. Wiklund, Vacuum, 32, 737, (1982).

18. S. Shanfield and M. Hendricks, Solid State Technology, 203, (1984).

19. D. HG. Choe, C. Knapp, and A. Jacob, Solid State Technology, 177, (1984).

20. F. D. Egitto, D. N. K. Wang, D. Maydan, and D. Benzing, Solid State Technology, 71, (1981)

21. J. W. Coburn and H. F. Winters, J. Vac. Sci.Technol., 16, 391, (1979).

22. H. W. Lehman and R. Windmer, J. Vac. Sci. Technol., 15, 319, (1978).

23. S. Matsuo, and Y. Takehara, Japan J. Appl. Phys., 16, 175, (1977).

24. M. M. Millard and E. Kay, J. Electrochem. Soc., 129, 160, (1982).

25. D. C. Gray, H. H. Sawin, and J. W. Butterbaugh, J. Vac. Sci. Technol., A9, 779, (1991).

26. G. Turban, Pure & Appl. Chem., 56, 215, (1984).

27. D. L. Flamm, V. M. Donnelly, and D. E. Ibbotson, J. Vac. Sci. Tech., B1, 23, (1983).

28. J. Dulak, B. J. Howard, and Ch. Steinbruchel, J. Vac. Sci. Tech. A9, 775,(1991)

29. "Modern Semiconductor Fabrication Technology," by P. Gise and R. Blanchard, Prentice Hall, New Jersey, 1986.

30. "Quick Reference Manual for Silicon IC Technology," edited by W. A. Beadle, J. C. C. Tsai, and R. D. Plummer, John Wiley & Sons, New York, 1985.

31. "Statistics for Experimenters," by G. E. P. Box, W. G. Hunter, and J. S. Hunter, John Wiley & Sons, New York, 1978.

32. XSTAT, Wiley Professional Software, John Wiley & Sons, Inc, New York.

33. "Design and Analysis of Experiments," by D. C. Montgomery, p. 546-547, 3rd Edition, John Wiley & Sons, 1991.

34. "Statistical Design and Analysis of Experiments," by P. W. M. John, The Macmillon Co., New York, 1971.

35. M. W. Jenkins, M. T. Mocella, K. D. Allen, and H. H. Swain, Solid State Technology, 175, (1986).

APPENDIX 1

Wafers with an oxide layer of known thickness and a resist pattern were immersed in buffered HF. The oxide etch rate was determined exactly by measuring the thickness after 5 minutes and 7 minutes of etch. The time to etch away the oxide layer was then calculated. The wafer was overetched for 1 hour after the removal of the oxide. Then, the resist was stripped away in a solution of resist stripper. This left a pattern of oxide on silicon. The oxide thickness was then reduced to about 1000 Å by etching with dilute HF. Dilute HF is known to etch silicon dioxide at a rate of about 160 Å/minute. Silicon is not etched by dilute HF. Oxide thickness was measured using NanoSpec. The step in the wafer was then measured using Alpha Step Profiler. The step is caused by the oxide layer and etched silicon. Thickness of etched silicon was calculated by subtracting the oxide thickness from the step measured by Alpha Step Profiler. The results are summarized in Table 1. The etch rate of silicon in buffered HF was about 2-3 Å/min.

Table 1. Etch Rate of Silicon in Buffered HF

Layer Measured	Thickness, Å				Mean Thickness Å
	1	2	3	4	
Oxide	1870	1875	1867	1866	1870
Si Step + Oxide	2010	1940	2020	1950	1980
Si*	140	65	153	84	110

* Si Etch Time= 60 min.
Hence, Si Etch Rate = 110/60 = 1.83 Å/min.

APPENDIX 2

CHRONOLOGY OF EXPERIMENTAL DESIGN AND DATA COLLECTION

A2.1. Response Surface Methodology 70
A2.2. Experimental Strategy 71
A2.3. Determination of Ranges for Process Variables 71
A2.4. Experiments to Fit First Order Model . . . 74
A2.5. Analysis of First Order Model 75
A2.6. Inadequacy of the First Order Model 77
A2.7. Experiments for Second Order Model 78
A2.7.1. Experiments along the Path of Steepest Ascent 78
A2.7.2. Alternate Strategy for Second Order Design 79
A2.7.3. Additional Experiments to Fit Second Order Model in the Range Settings Given in Table 2 81
A2.8. Determination of Conditions for Maximum Selectivity 81
A2.9. Experiments at Standard Conditions 82
A2.10. Power Consumption - The Cause of Increased Etch Rates 83
A2.11. Estimation of the Correction Factor 84
A2.12. Experiments in the Expanded Reaction Surface 85

APPENDIX 2
CHRONOLOGY OF EXPERIMENTAL DESIGN AND DATA COLLECTION

The experiments were designed initially using the Response Surface Methodology, RSM. Due to polymerization, complications arose in the characterization of the reaction surface. This Appendix describes the experimental strategy adopted in this study to circumvent the difficulties.

A2.1. Response Surface Methodology

Since our aim was to get optimum selectivity in SiO_2 etching with respect to Si etching RSM was chosen for the design of experiments. Response surface methodology is a statistical approach used to maximize or minimize a response controlled by several variables[31]. In the RSM approach, a finite number of experiments are carried out according to a preset experimental design. The number of process parameters determine the number of experiments that are needed for obtaining the analytical response surfaces.

Determination of the experimental ranges for the variables, designing a set of experiments to fit a first order equation, determining the path of steepest ascent for selectivity in oxide etching and performing experiments along this path, and designing and conducting experiments

around the maximum selectivity to fit a second degree polynomial are the various stages in the design of experiments.

A2.2. Experimental Strategy

Initial ranges were set, a first order design was developed, and the experiments were conducted in accordance with the strategy described in the previous section. However, as will be seen in the following sections, the responses could not be fit using a first order design. Attempts to reach a point close to the maximum in selectivity by using the approximate path of steepest ascent also failed. It was not possible to use the conventional designs to obtain more data points for a second order fit and to span as much of the reaction surface as possible. Hence, experiments in the expanded reaction surface and close to the polymer point were chosen randomly. The logistics of the choice of experimental conditions, and the results obtained are discussed in detail in the following sections.

A2.3. Determination of Ranges for Process Variables

In our study, DC bias, pressure, and flow rates of CHF_3, CH_4, and O_2 were the process variables. In order to determine the experimental ranges, preliminary experiments listed in Table 1 were conducted.

Table 1. Experiments to Determine Variable Ranges

Run No.	DC Bias, V (X1)	Press-ure, mT (X2)	CHF_3 Flow, sccm (X3)	CH_4 Flow, sccm (X4)	O_2 Flow, sccm (X5)	SiO_2 Etch Rate, Å/min (Y1)
I-1	-500	40	75	3	2	P*
I-2	-700	30	80	6	2	64#
I-3	-700	30	80	6	4	321#
I-4	-700	50	80	6	4	510
I-5	-500	50	80	10	10	P*
I-6	-600	30	80	10	10	P*
I-7	-700	30	80	10	10	206#
I-8	-600	30	80	8	12	420
I-9	-500	30	80	8	12	36#

* P - Polymer Deposition; # - Nonuniform Etching

For run 1, DC bias, pressure, and CHF_3 flow rates were chosen near the center of the ranges of interest mentioned in Table 2. Since oxygen addition is known to decrease the selectivity in oxide/silicon etching, oxygen flow rate was chosen to be closer to the lower end of the range. In order to minimize the adverse reactions, if any, between oxygen and methane in the plasma, methane flow rate was also chosen to be near the lower end of the range in run 1. This set of conditions led to polymer deposition and was observed by the increase in SiO_2 thickness.

Attempts at attaining a pressure of 60 mT at bias values between -500 - -700 V led to arcing in the chamber irrespective of the presence of O_2. Moreover, a bias of over -700 V was not maintainable at pressures greater than 50 mT. This led to the lowering of the upper limits aimed for bias and pressure to -700 V and 60 mT respectively.

Run 2 was carried out at -700 V and 30 mT and a methane flow rate of 6 sccm. The oxide etching was minimal and highly nonuniform; the thickness varied as much as 500 Å across the wafer. Oxygen flow was increased in run 3 which resulted in oxide etching at a rate of about 320 Å/min. However, the uniformity in etching was poor. That is, the oxide thickness varied across the surface by over 5%. An increase in pressure from 30 to 50 mT in run 4 resulted in more uniform etching of the oxide and higher etch rate. From these set of experiments it was thought that in the presence of methane a decrease in pressure leads to lower SiO_2 etch rates and etching uniformities.

Runs 5, 6, and 7 were run at 10 sccm of CH_4 and O_2 flow rates and at -500, -600 and -700 V of bias respectively. In runs 5 and 6 polymer deposition was observed while in run 7 etching was nonuniform. Hence, experiments 8 and 9 were run with CH_4 and O_2 flows of 8 and 12 sccm respectively; that

is, under reduced methane and increased oxygen flows. In run 8, at a bias of -600 V, the oxide etching was reasonably uniform (thickness variation across the wafer was <5%). Whereas, in run 9 at -500 V and 30 mT, the etching was nonuniform and extremely slow (about 60 Å/min.).

Based on the above experiments variable settings shown in Table 2 were chosen for the first order design.

Table 2. Variable Settings for First Order Design

Setting	DC Bias, V	Pressure mT	CHF_3 Flow Rate, sccm	CH_4 Percent	O_2 Percent
-1, Low	-600	30	50	0	9
0, Middle	-650	40	75	3	12
1, High	-700	50	100	6	15

A2.4. Experiments to Fit First Order Model

A 2^{k-1} fractional factorial design with three replicates was chosen for the first order design. This involved 19 experiments as given in Table 3.

The wafers were etched under the conditions specified in Table 3 and the etch rates of SiO_2, Y1, and silicon, Y2, were determined. Table 4 lists the SiO_2 and Si etch rates and the selectivity of oxide etch, Y3, for these runs.

Table 3. Fractional Factorial Design for Five Variables[a]

No.	DC Bias, V	Pressure mTorr	CHF_3 Flow, cc	CH_4 Percent	O_2 Percent
1	-1	-1	-1	-1	1
2	-1	-1	-1	1	-1
3	-1	-1	1	-1	-1
4	-1	-1	1	1	1
5	-1	1	-1	-1	-1
6	-1	1	-1	1	1
7	-1	1	1	-1	1
8	-1	1	1	1	-1
9	1	-1	-1	-1	-1
10	1	-1	-1	1	1
11	1	-1	1	-1	1
12	1	-1	1	1	-1
13	1	1	-1	-1	1
14	1	1	-1	1	-1
15	1	1	1	-1	-1
16	1	1	1	1	1
17	0	0	0	0	0
18	0	0	0	0	0
19	0	0	0	0	0

@ - The actual experimental order was not the same as above.

A2.5. Analysis of First Order Model

The fit of the data given in Table 8 to a first degree polynomial **Response** = $a_0 + \Sigma\, a_i x_i + \epsilon$ was checked using the interaction and curvature terms[31] listed in Table 5. The average is a_0, a_is are the main effects (i.e., the

slopes in the five directions) and ϵ is the standard error. In these calculations all the x_i axes were normalized (i.e., -1 to +1).

Table 4. Etch Rates and Selectivities for the First Order Fit

No.	Run No.	X1, -V	X2, mT	X3, sccm	X4, sccm	X5, sccm	Y1, Å/mi	Y2, Å/mi	Y3
1	13	600	30	50	0	15	318	246	1.29
2	5	600	30	50	6	9	342	18	19.0
3	10	600	30	100	0	9	423	55	7.69
4	2	600	30	100	6	15	400	40	10.0
5	16	600	50	50	0	9	540	110	4.91
6	4	600	50	50	6	15	491	76	6.46
7	11	600	50	100	0	15	608	127	4.79
8	19	600	50	100	6	9	336	21	16.0
9	7	700	30	50	0	9	489	121	4.04
10	14	700	30	50	6	15	435	72	6.04
11	3	700	30	100	0	15	552	104	5.31
12	17	700	30	100	6	9	462	30	15.4
13	9	700	50	50	0	15	650	178	3.65
14	8	700	50	50	6	9	567	71	7.99
15	15	700	50	100	0	9	670	91	7.36
16	1	700	50	100	6	15	649	82	7.91
17	6	650	40	75	3	12	547	94	5.82
18	12	650	40	75	3	12	552	91	6.07
19	18	650	40	75	3	12	532	84	6.33

The a_0, a_i s, and ϵ calculated for the response Y3, namely, the selectivity are reported in Table 9. Also reported are

the interaction between the variables, i.e., a_{ij}s and the overall curvature, i.e., the sums of the a_{ii}s.

Table 5. First Order Analysis for Selectivity

Average:		
a_0	=	7.68
Main Effects:		
a_1	=	-0.7775
a_2	=	-0.6063
a_3	=	1.3175
a_4	=	3.1100
a_5	=	-2.3088
Standard Error:		
ϵ	=	0.2327
Interactions:		
a_{12}	=	0.1213
a_{13}	=	0.4650
a_{14}	=	-0.9875
a_{15}	=	0.8238
a_{23}	=	0.3138
a_{24}	=	-0.9038
a_{25}	=	0.6275
a_{34}	=	-0.0900
a_{35}	=	0.0038
a_{45}	=	-1.1888
Curvature:		
$\Sigma\ a_{ii}$	=	1.95

A2.6. Inadequacy of the First Order Model

Since the interaction and curvature terms given in Table 5 are quite significant with respect to the standard error, it

can be concluded that the first order model is inadequate. The data in Table 4 were analyzed by XSTAT[32] using the linear regression method for all the three responses, namely, etch rates of SiO_2 and Si. The variations about the mean as given by the R- squared values are:

SiO_2 Etch Rate = 81.4 %

Si Etch Rate = 79.6 %

Selectivity = 77.3%

The R-squared values also indicate the lack of fit for the first order model for all the three responses. The first order model will be able to represent the response away from the maxima/ minima and will fail close to the extremas[33]. The failure of the first order model suggests that the optima are not far away from the set variable ranges. Hence, a higher order model is necessary to fit the data.

A2.7. Experiments for Second Order Model

A2.7.1. Experiments along the Path of Steepest Ascent:

As discussed in the previous section, the extremas are not too far away from the variable ranges studied. In order to obtain the conditions close to the optimum in selectivity, experiments should be conducted along the path of steepest ascent. Though the first order fit was poor, it was thought necessary to obtain a point close to the optimum for designing the experiments to fit the second order model.

Two of the experimental conditions chosen along the path of steepest ascent using the coefficients listed in Table 5 are run numbers 20 and 21 listed in Table 6. A selectivity of 17.64 was obtained from run 20. However, in Run 21, the oxide etching was nonuniform and measurement of Si etch rate was not possible due the nonuniformity of the wafer surface. This is probably due to the fact that oxygen content in the gas mixture is too low to effectively remove the hydrocarbon and fluorocarbon radicals, the polymer precursors, deposited on the wafer surface. A low oxide etch rate (230 Å/min in comparison with about 400 Å/min or higher obtained under similar conditions of bias, power and CHF_3 flow rate) can be considered to support this argument.

Table 6. Experiments Along the Path of Steepest Ascent

No.	Run No.	X1, -V	X2, mT	X3, sccm	X4, sccm	X5, sccm	Y1, A/mi	Y2, A/mi	Y3
20	20	637	37	89	7	10	441	25	17.6
21	21	625	35	96	9	8	230	-	-

A2.7.2. Alternate Strategy for Second Order Design:

Failure of experiment 21 to produce the data inhibits the use of steepest ascent method to reach close to the optimum in selectivity. Another approach to the conditions for optimum selectivity is to augment the runs chosen for the first order design using the central composite design[34],

CCD, so that a second degree polynomial could be fit. The additional data points required by the central composite design are called the star points. For a five variable system these star points are a set of 10 axial points at a distance 2 from the origin as illustrated in Table 7.

Table 7. Star Points for Second Order Fit by CCD

Number	X1	X2	X3	X4	X5
1	+2	0	0	0	0
2	-2	0	0	0	0
3	0	+2	0	0	0
4	0	-2	0	0	0
5	0	0	+2	0	0
6	0	0	-2	0	0
7	0	0	0	+2	0
8	0	0	0	-2	0
9	0	0	0	0	+2
10	0	0	0	0	-2

However, the use of CCD to augment the data collected in the ranges given in Table 2 to fit the first order model would require experiments to be performed at unattainable conditions, namely, -750 V bias and 40 mT pressure, -650 V bias and 60 mT pressure, and CH_4 flow rate of -3 sccm corresponding to the star points 1, 3 and 8 of Table 11 respectively. (Conditions corresponding to the star point 1 and 3 are not attainable due to instrument limitations.)

A2.7.3. Additional Experiments to Fit Second Order Model in the Range Settings Given in Table 2:

Since the first order analysis indicated that the maximum in selectivity is not far from the experimental ranges given in Table 2, additional experiments are either conducted under conditions within or close to these ranges. These experiments and the results obtained from them are presented in Table 8.

Table 8. Additional Experiments for Second Order Fit

No.	Run No.	X1, -V	X2, mT	X3, sccm	X4, sccm	X5, sccm	Y1, Å/mi	Y2, Å/mi	Y3
1	20	637	37	89	7	10	441	25	17.6
2	22	710	40	75	3	12	658	152	4.33
3	23	640	40	75	3	12	515	82	6.28
4	24	600	30	85	6	9	361	15	24.1
5	25	600	30	80	8	12	420	40	10.5
6	26	700	30	85	6	9	552	63	8.76

A2.8. Determination of Conditions for Maximum Selectivity

In order to find the conditions for optimum selectivity, the optimization routine in XSTAT was used. The starting factor values for the maximization of the selectivity were -650 V bias, 40 mT pressure, 75 sccm CHF_3, 3 sccm CH_4, and 10 sccm O_2. The optimum was calculated to be at -600 V bias, 42 mT pressure, 93.9 sccm CHF_3, 6.0 sccm CH_4, and 8.6 sccm O_2. The

expected selectivity under these conditions was 26.9. Occurrence of the optimum at -600 V bias, i.e., at the lower limit of the range suggests that a lower bias might lead to an increase in selectivity. Moreover, it is advantageous to cover as much of the reaction surface as possible to characterize the surface.

The reaction surface that can be studied using the Design of Experiments technique is limited because:

(i) Some combinations of bias and pressure settings required by the DOE were unattainable due to instrument limitations.

(ii) Some combinations of flow rates were not possible due to polymer deposition.

Hence, in order to cover as much of the reaction surface as possible, additional experiments were conducted at conditions not conforming to the DOE technique.

A2.9. Experiments at Standard Conditions

The standard conditions suggested by the instrument manufacturer for oxide etching are:

Bias	=	-575 V
Pressure	=	45 mT
CHF_3 Flow	=	75 sccm
O_2	=	8 sccm .

Under these conditions, i.e. in run 27, the oxide etch rate was obtained to be 514 Å, about 50-60 Å higher than the normal etch rate of about 460 Å obtained under identical conditions. The experiment was repeated (run 28) in order to verify the reproducibility. The oxide and silicon etch rates were found to be higher in both the runs. It was thought to be necessary to analyze the cause of the discrepancy.

A2.10. Power Consumption - The Cause of Increased Etch Rates

In order to find out the cause of the discrepancy in etch rates, etching was done at -650 V bias, 40 mT pressure, 75 sccm CHF_3, 3 sccm CH_4, and 12 sccm O_2, the conditions under which three sets of data points are available. The oxide etch rate observed in this case, i. e., in run 29, was 634 Å/min, about 90 Å/min higher than the average value obtained from runs 6, 12 and 18 (refer Table 4). It was noted that the power required to maintain the bias is about 200 W higher in the case of run 29. Similarly, in runs 27 and 28, the observed power was 1300 W, about 125 W higher than the normally observed power level of 1160 W. The observed power values for all the experiments are presented in Appendix 3.

It was thought that cleaning the reaction chamber might

bring the power back to the original values. The drop in power after the clean up operation was only momentary. Investigation by Applied Materials, the instrument manufacturer, did not lead to any solution. Since the cause of the jump in power requirement could not be pin pointed, it became necessary to apply a correction factor to the data obtained in subsequent experiments. It is worth mentioning at this point that similar power variations were observed earlier in our laboratories but no change was noticed in the etch rates.

A2.11. Estimation of the Correction Factor

The equilibrium power values recorded during the runs listed in Tables 1, 4, 6, and 8 were fitted with a second degree polynomial using XSTAT. Since power fluctuations were considerable during many runs, the fit was not excellent. The R-squared term was only 95%. The fit was improved by discarding the data points with high residuals. The resultant correlation was excellent with an R-squared term of 99.9%. Using the regression equation thus developed the expected power values were obtained for runs 27 and higher.

Corrections factors for SiO_2 and Si etch rates listed in Table 9 were derived as a function of the power variation using the data available under the experimental conditions

of runs 27 and 29. The experiments and the observed power values utilized in the development of the regression equation are tabulated in Appendix 4.

Table 9. Determination of Correction Factors

Set*	Run No.	Power	SiO_2 Etch Rate,A/min	SiO_2 Corr. Factor, $\alpha^{@,!}$	Si Etch Rate, A/min.	Si Corr. Factor, $\beta^{@,\#}$
I	6,12&18	1359	544	$\frac{P_e}{P_o}$	90	$\frac{1.08P_e}{P_o}$
	29	1565	634		96	
II	Std.	1160	458	$\frac{P_e}{P_o}$	68.2	$\frac{1.073P_e}{P_o}$
	27 & 28	1300	514		71.7	

* - Experimental Conditions:
Set I = -650 V, 40mT, & 75, 3, & 12 sccm flows
Set II = -575 V, 45 mT, & 75, 0, & 8 sccm flows
@ - P_e = Power estimated; P_o = Power observed
! - The ratio of etch rates = The ratio of power.
- The ratio of etch rates = 1.076 times the ratio of powers
β = Average of the two values = $1.076 \times P_e / P_o$.

A2.12. Experiments in the Expanded Reaction Surface

The observed power and etch rates for the runs 27 and higher are given in Table 10. This data set represents the reaction surface in the expanded range and outside the limits explored using the DOE technique. The corrected power was obtained using the regression equation for power.

The oxide etch rates were corrected by multiplying the observed etch rate with α. Si etch rates were corrected by

multiplying with the factor ß which is the average of the two values reported in Table 9. Table 11 provides the corrected power and etch rates for these experiments.

Table 10. Data for the Expanded Reaction Surface

No.	Run No.	X1, -V	X2, mT	X3, sccm	X4, sccm	X5, sccm	Pow-er,W	Y1, Å/mi	Y2, Å/mi
1	27	575	45	75	0	8	1300	514	74
2	28	575	45	75	0	8	1290	513	69
3	29	650	40	75	3	12	1565	634	96
4	30	575	45	75	3	8	1300	473	51
5	31	575	45	75	5	8	1340	370	25
6	32	575	35	75	3	5	1160	391	27
7	33	575	45	75	3	5	1300	450	45
8	34	575	45	75	0	5	1328	510	61
9	35	750	20	50	6	9	1210	385	30
10	36	650	40	75	3	12	1500	596	87
11	37	500	50	75	6	9	1085	30*	-*
12	38	800	20	50	6	9	1479	462	38
13	39	550	35	50	6	9	1024	324	15
14	40	550	20	50	6	9	820	243	28
15	41	650	20	50	6	9	1052	330	23
16	42	500	30	75	3	8	895	322	37
17	43	750	30	100	6	9	1720	580	41
18	44	550	40	91	1	5	1185	438	88

* -Nonuniform etching of SiO_2; Si etch rates could not be measured.

The corrected data provided in Table 11 is used in the second order regression analysis for the expanded reaction

surface. The analysis in the narrow range and the expanded range are provided in the next chapter.

Table 11. Observed and Corrected Data for Runs Listed in Table 10

No.	Run No.	Power, W		SiO_2 Etch Rate,Å/min		Si Etch Rate,Å/min		Selecti-vity	
		Obs.	Cor.	Obs.	Cor.	Obs.	Cor.	Obs.	Cor.
1	27	1300	1161	514	459	74	71	6.95	6.46
2	28	1290	1161	513	459	69	67	7.43	6.90
3	29	1565	1358	634	550	96	90	6.60	6.11
4	30	1300	1013	473	369	51	43	9.27	8.58
5	31	1340	965	370	266	25	19	14.8	14.0
6	32	1160	945	391	319	27	24	14.5	13.3
7	33	1300	954	450	330	45	36	10.0	9.17
8	34	1328	1210	510	465	61	60	8.36	7.75
9	35	1210	1227	385	385	30	30	12.9	12.9
10	36	1500	1358	596	540	87	85	6.85	6.21
11	38	1479	1465	462	458	38	38	12.2	12.1
12	39	1024	955	324	302	15	15	21.6	20.1
13	40	820	602	243	178	28	22	8.68	8.09
14	41	1052	785	330	246	23	18	14.3	13.7
15	42	895	644	322	232	37	29	8.70	8.00
16	43	1720	1627	580	549	41	41	14.1	13.4
17	44	1185	963	438	356	88	77	4.98	4.62

APPENDIX 3

Table 1. Observed Power in the RIE Experiments

Run No.	Power, W	Run No.	Power, W	Run No.	Power,W
I-1	-	I-2	1315	I-3	1316
I-4	1589	I-5	957	I-6	1038
I-7	1280	I-8	1167	I-9	882
1	1780	2	1080	3	1415
4	1265	5	1051	6	1360
7	1400	8	1630	9	1700
10	1050	11	1400	12	1366
13	1100	14	1345	15	1790
16	1300	17	1370	18	1350
19	1300	20	1340	21	1275
22	1790	23	1300	24	1155
25	1167	26	1510	27	1300
28	1290	29	1565	30	1300
31	1340	32	1160	33	1300
34	1328	35	1210	36	1500
37	1085	38	1479	39	1024
40	820	41	1052	42	895
43	1720	44	1185	-	-

APPENDIX 4

Table 1. Power Correlation

#	X1	X2	X3	X4	X5	POWER
1	700.0	30.00	80.00	6.00	2.00	1315.0
2	700.0	30.00	80.00	6.00	4.00	1316.0
3	500.0	50.00	80.00	10.00	10.00	957.0
4	600.0	30.00	80.00	10.00	10.00	1038.0
5	700.0	30.00	80.00	10.00	10.00	1325.0
6	500.0	30.00	80.00	8.00	12.00	882.0
7	688.0	50.00	35.00	6.00	9.00	1775.0
8	600.0	30.00	100.00	6.00	15.00	1080.0
9	688.0	50.00	100.00	6.00	15.00	1780.0
10	600.0	50.00	50.00	6.00	15.00	1265.0
11	600.0	30.00	50.00	6.00	9.00	1051.0
12	650.0	40.00	75.00	3.00	12.00	1360.0
13	700.0	50.00	50.00	0.00	15.00	1700.0
14	600.0	30.00	100.00	0.00	9.00	1050.0
15	650.0	40.00	75.00	3.00	12.00	1366.0
16	600.0	30.00	50.00	0.00	15.00	1100.0
17	700.0	30.00	50.00	6.00	15.00	1345.0
18	675.0	50.00	100.00	0.00	9.00	1780.0
19	700.0	30.00	100.00	6.00	9.00	1370.0
20	650.0	40.00	75.00	3.00	12.00	1350.0
21	600.0	50.00	100.00	6.00	9.00	1300.0
22	575.0	45.00	75.00	0.00	8.00	1160.0
23	640.0	40.00	75.00	3.00	12.00	1300.0
24	637.0	37.00	89.00	7.00	10.00	1340.0
25	625.0	36.00	96.00	9.00	8.00	1275.0